

Characterization of Small Antennas & Wireless Devices for MIMO Systems in Multipath & Line-of-Sight

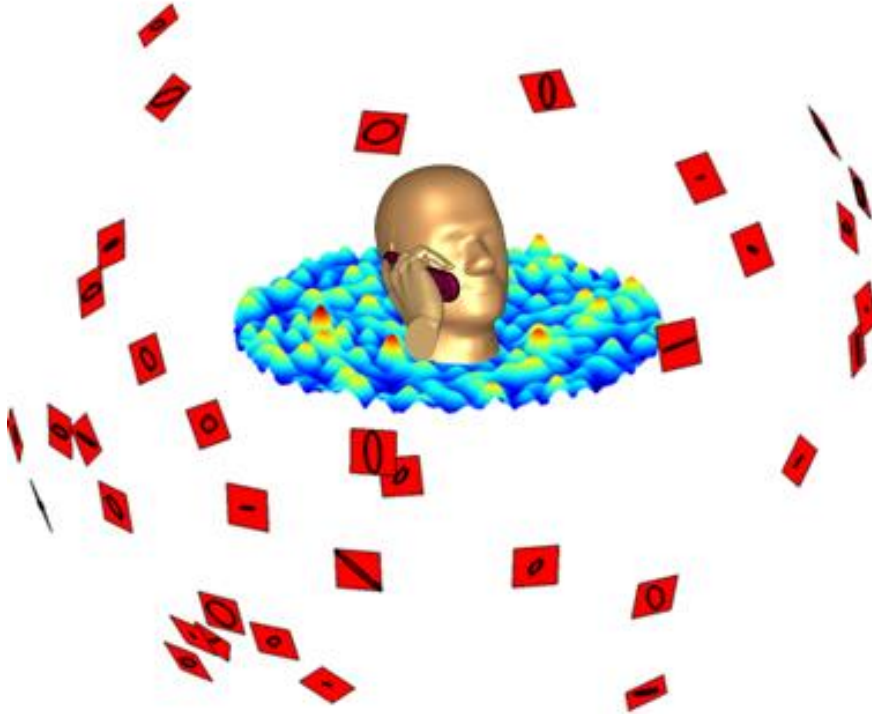
AHMED HUSSAIN

Department of Signals and Systems
CHALMERS UNIVERSITY OF TECHNOLOGY
Gothenburg, Sweden 2014

AHMED HUSSAIN

Characterization of Small Antennas & Wireless Devices
for MIMO Systems in Multipath & Line-of-Sight

2014



Characterization of Small Antennas & Wireless Devices for MIMO Systems in Multipath & Line-of-Sight

AHMED HUSSAIN

Department of Signals and Systems
CHALMERS UNIVERSITY OF TECHNOLOGY
Gothenburg, Sweden 2014

THESIS FOR THE DEGREE OF DOCTOR OF PHILOSOPHY

Characterization of Small Antennas & Wireless Devices
for MIMO Systems in Multipath & Line-of-Sight

by

AHMED HUSSAIN



CHALMERS

Division of Antenna Systems
Department of Signals and Systems
Chalmers University of Technology
SE-41296 Göteborg, Sweden

August 2014

Characterization of Small Antennas & Wireless Devices for MIMO Systems in Multipath & Line-of-Sight

AHMED HUSSAIN

Copyright © AHMED HUSSAIN, 2014
All rights reserved

ISBN 978-91-7597-057-8

ISSN 0346-718X

Series No. 3738

Division of Antenna Systems

Department of Signals and Systems

Chalmers University of Technology

SE – 412 96 Göteborg, Sweden

Telephone: +46 (0) 31 772 1000

Contact information:

Ahmed Hussain

Department of Signals and Systems

Chalmers University of Technology

SE – 412 96 Göteborg, Sweden

Telephone: +46 (0) 31 772 1933

Email: ahmed.hussain@chalmers.se

Printed in Sweden by Chalmers Reproservice
Göteborg, Sweden, August, 2014

To my family & friends

Abstract

The current thesis investigates over-the-air (OTA) performance characterization of small antennas and wireless terminals in rich isotropic multipath (RIMP) environment, as well as in pure line-of-sight (LOS) environment when taking into account the random positions and orientations of the mobile terminals caused by the realistic user behavior. The latest mobile wireless terminals such as smart phones and tablets can be used in any random orientation thereby making even a received LOS-component appear as a random voltage at the antenna ports over time. The terms "RIMP" and "Random-LOS" are coined to represent the two limiting environments for OTA performance characterization of mobile terminals. In practice, RIMP environment can be emulated using reverberation chambers while the LOS environment can be emulated using anechoic chambers. Mobile terminals are mostly used in indoor multipath environments, e.g. homes, offices and shopping malls. Therefore the main focus of this thesis is on measuring and simulating OTA performance of small antennas and wireless devices in RIMP environment. The paper [A1] is related to using RIMP as a reference environment, and contains a study of the comparison between 2D and 3D multipath environments for single-port and multi-port antennas.

Recently, the OTA testing of 4G Long Term Evolution (LTE) devices has become very important in order to characterize the implemented Multiple-Input Multiple-Output (MIMO) and Orthogonal Frequency Division Multiplexing (OFDM) technologies. Features such as adaptable modulation scheme, system bandwidth, coding rate, and diversity have made communication system more robust and adaptable to the environment. We introduced in 2011 a new theory based on an ideal threshold receiver in order to model the Total Isotropic Sensitivity (TIS) and the OTA throughput of LTE devices including their diversity gains due to MIMO and OFDM. This model was later tested for different LTE system bandwidths and coherence bandwidths in papers [B1-B3], and it has shown to give very good agreement with measurements in RIMP.

Measuring and modeling the OTA performance of the latest wireless commercial devices have always been interesting. However, such commercial devices are often a black box and most of the technical details are kept as business secrets. Under such circumstances, we benefit from the Universal Software Radio Peripheral (USRP) which is an inexpensive and flexible Software Defined Radio (SDR). It provides a radio platform to design a reliable communication link where all important settings such as modulation, frequency, sampling rate, antenna gain, etc. are defined on software by the user. The USRPs are good alternatives to both devices-under-test (DUTs) as well as measurement instruments. For the first time, we demonstrate that USRPs can measure both active and passive OTA performance inside the reverberation chamber in papers [C1, C2].

The OTA performance characterization of single-port mobile terminals has been studied for several years now. Today, LTE mobile terminals are equipped with multipoint antennas which must be characterized for OTA environments. The study of OTA performance characterization of a two-port mobile phone mockup on both sides of the head following standardized talk positions is presented in papers [D1, D2].

At Chalmers University, a unique multiport ultra-wideband (UWB) self-grounded bow-tie antenna has been designed and developed during the last few years. The OTA performance characterization of this antenna has been completed by measurements and simulations in RIMP environment. The results are presented in papers [E1, E2].

The OTA performance of compact UWB antennas designed for mobile phone applications at Linköping University, Sweden, and for body-centric wireless communications at École polytechnique fédérale de Lausanne (EPFL), Switzerland are presented in papers [F1, F2]. A unique study comparing drive test measurements and reverberation chamber measurements is presented in paper [F3]. Another interesting paper which introduces a new real-life OTA measurement method to improve cellular network performance is appended as paper [F4].

During the last decade, several multipath environment models and simulation tools have been developed. Similarly, Rayleigh-lab and ViRM-lab are developed at Chalmers University to study convergence and validation of efficiency, correlation, and diversity gain measurements in reverberation chamber. Moreover, we can also compare different multipath environments as well as different devices in different environments. This thesis presents some results based on these simulation tools which show excellent agreement with the measurements. The description of these simulation tools with some examples is presented in papers [G1, G2].

Keywords: OTA, LOS, RIMP, LTE, MIMO, SDR, USRP, TIS, TRP, Throughput, Rayleigh, Reverberation chamber.

Preface

This report is a thesis for the degree of Doctor of Philosophy at Chalmers University of Technology. This work has been carried out between October 2009 and October 2014 at the Antenna Group, Department of Signals and Systems, Chalmers University of Technology. Professor Per-Simon Kildal has been the main supervisor as well as the examiner and Professor Jan Carlsson has been the co-supervisor.

This work has been financially supported in part by The Swedish Governmental Agency for Innovation Systems (VINNOVA) within the VINN Excellence Center Chase, and by Swedish Strategic Research Foundation (SSF) within the Chalmers Microwave Antenna Systems Research Center (CHARMANT).

Acknowledgements

I would like to especially acknowledge my supervisor Prof. Per-Simon Kildal for giving me an exciting opportunity to study for a PhD degree and work at Chalmers University of Technology. I am very thankful to you for creating jolly and positive atmosphere through your sense of humor, emotions, energy and passion which you dedicate to your work. Your innovative ideas, commercialization, encouragement and appreciation helped me to work restlessly on different interesting projects. I'm honored to be a part of your group.

I would like to give my special thanks to Prof. Jan Carlsson and Dr. Ulf Carlberg for their supervision, collaboration, and fruitful discussions. I would like to acknowledge all co-authors to my publications for their contribution and cooperation.

I would also like to appreciate the antenna family for organizing activities and developing a very homely atmosphere in the corridor. Thank you all: Prof. Ahmed, Abbas, Aidin, Ali, Ashraf, Astrid, Bjarni, Carlo, Elena, Eric, Esperanza, Prof. Eva, Hasan, Prof. Jian, Madeleine, Prof. Marianna, Nima, Oleg, Prof. Rob, Sofia, Weiming, and Xiaoming. I would like to thank all of my colleagues and friends at S2 department for great cooperation and joyful environment. I am also thankful to Helene and Jingya; it was fun to learn Swedish language with you. I would like to acknowledge administration and management staff at the university.

I would like to give a big thanks to my friends: Abid, Anum, Banaz, Dan, Elena, Hasan, Kristin, Malin, Mari, Matilda, Nasser, Nima, Noelia, Olga, Sadia, Sajana, Umair, Waqar, and all others. I cannot be more thankful to my friendly neighbors at SGS Viktor Rydbergsgatan - you have been the biggest support to me at all times. Living quite far from my culture, family, food, and traditions would have been hard without your true friendship and support.

I would also like to thank all managers and active contributors involved in CHASE projects and especially SP, Bluetest, Sony, Telenor, and Ericsson for their contributions. I would like to thank Swedish Governmental Agency for Innovation Systems (VINNOVA) for creating research opportunities by financial support to scientific and technological development in society. I am greatly thankful to Chalmers University for providing the best teaching and learning environment with all resources at the institution. I am also thankful to the students in the antenna engineering course to nominate me for Chalmers Pedagogic Award in 2010, which I received.

I want to acknowledge my family and especially my life's first teacher – my mom – for all the efforts she put on me to become what I am today. I want to acknowledge all of my teachers and supervisors for giving me exciting opportunities to work and learn from them. I want to acknowledge Madiha for being a big moral support to me during the last year of this journey. Last, but not the least, I am extremely thankful to Almighty God for everything I have in life!

Ahmed Hussain
Gothenburg, August 2014.

List of Papers

- A1.** J. Carlsson, U. Carlberg, **A. Hussain**, P. Kildal, "About Measurements in Reverberation Chamber and Isotropic Reference Environment," presented at the 20th International Conference on Applied Electromagnetics and Communications (ICECom), September 2010.
- B1.** P. Kildal, **A. Hussain**, X. Chen, C. Orlenius, A. Skårbratt, J. Åsberg, T. Svensson, T. Eriksson, "Threshold Receiver Model for Throughput of Wireless Devices With MIMO and Frequency Diversity Measured in Reverberation Chamber," *IEEE Antennas and Wireless Propagation Letters (IEEE-AWPL)*, vol. 10, pp. 1201-1204, November 2011.
- B2.** **A. Hussain** and P. Kildal, "Study of OTA Throughput of LTE Terminals for Different System Bandwidths and Coherence Bandwidths," presented at the 7th European Conference on Antennas and Propagation (EuCAP), April 2013.
- B3.** **A. Hussain** and P. Kildal, "Replacing TIS by OTA Throughput for Measuring Receiver Quality of SISO & MIMO LTE Terminals in Reverberation Chambers," manuscript submitted to *IEEE Transactions on Antennas and Propagation (IEEE-TAP)*, June 2014.
- C1.** **A. Hussain**, B. Einarsson, P. Kildal, "MIMO OTA Testing of Communication System Using SDRs in Reverberation Chamber," manuscript submitted to *IEEE Antennas & Propagation Magazine*, July 2014.
- C2.** **A. Hussain**, B. Einarsson, P. Kildal, "Antenna Measurements in Reverberation Chamber Using Software Defined Radio," manuscript to be submitted to *IEEE Antennas and Wireless Propagation Letters (IEEE-AWPL)*, August 2014.
- D1.** **A. Hussain** and P. Kildal, U. Carlberg, J. Carlsson, "Diversity Gains of Multiport Mobile Terminals in Multipath for Talk Positions on Both Sides of the Head," presented at the 7th European Conference on Antennas and Propagation (EuCAP), April 2013.
- D2.** **A. Hussain** and P. Kildal, "Correlation Between Far-field Patterns on Both Sides of the Head of Two-port Antenna on Mobile Terminal," presented at International Symposium on Antennas and Propagation (ISAP), October 2013.
- E1.** Al-Rawi, **A. Hussain**, J. Yang, M. Franzen, C. Orlenius, "A New Compact Wideband MIMO Antenna – The Double-sided Tapered Self-grounded Monopole Array," *IEEE Transactions on Antennas and Propagation (IEEE-TAP)*, vol.62, pp. 3365-3369, June 2014.
- E2.** H. Raza, **A. Hussain**, J. Yang, P. Kildal, "Wideband Compact 4-port Dual Polarized Self-grounded Bowtie Antenna," accepted for publication in *IEEE Transaction on Antennas and Propagation (IEEE-TAP)*, June 2014.
- F1.** M. Koohestani, **A. Hussain**, A. Moreira, A. Skrivervik, "Diversity Gain Influenced by Polarization and Spatial Diversity Techniques in UWB", submitted to *International Journal of RF and Microwave Computer-Aided Engineering*, July 2014.
- F2.** M. Asghar, M. Malick, M. Karlsson, **A. Hussain**, "A Multi-wideband Planar Monopole Antenna for 4G Devices", *Microwave and Optical Technology Letters*, vol. 5, pp. 589-593, 2013.

- F3.** H. J. Song, A. Bekaryan, J. H. Schaffner, **A. Hussain**, P. Kildal, "Effects of Mutual Coupling on LTE MIMO Capacity for Monopole Array: Comparing Reverberation Chamber Tests and Drive Tests," accepted for publication in IEEE Antennas and Wireless Propagation Letters (IEEE-AWPL), May 2014.
- F4.** P. Hjalmar, P. Gronsund, K. Mahmood, P. Kildal, X. Chen, **A. Hussain**, K. Arvidsson, J. Carlsson, "Using User-submitted OTA Measurements Obtained From the Handset to Determine Performance of its Antenna and the Network," presented at the European Cooperation in the Field of Scientific and Technical Research – COST IC1004, February 2014.
- G1.** P. Kildal, **A. Hussain**, U. Carlberg, J. Carlsson, "On Using Isotropic Multipath as Reference Environment for OTA Performance: Uncertainty due to Convergence of Statistical Expectation when Estimating Ergodic Capacity and Diversity Gain," presented at the European Cooperation in the field of Scientific and Technical Research - COST2100, June 2010.
- G2.** U. Carlberg, P. Kildal, **A. Hussain**, J. Carlsson, "On Using Isotropic Multipath as Reference Environment for OTA Performance: Ray-based Multipath Simulation Tool for Studying Convergence and Uniqueness of Different User-related Statistical Expectations when Estimating Ergodic Capacity and Diversity Gain," presented at the European Cooperation in the field of Scientific and Technical Research - COST2100, June 2010.

Other publications:

- **A. Hussain**, P. Kildal, J. Carlsson, "Uncertainties in Estimating Ergodic MIMO Capacity and Diversity Gain of Multiport Antenna Systems with Different Port Weights," presented at the 5th European Conference on Antennas and Propagation (EuCAP), April 2011.
- **A. Hussain**, U. Carlberg, J. Carlsson, P. Kildal, "Analysis of Statistical Uncertainties Involved in Estimating Ergodic MIMO Capacity and Diversity Gain in Rayleigh Fading Environment," presented at the 20th International Conference on Applied Electromagnetics and Communications (ICECom), September 2010.
- **A. Hussain**, P. Kildal, U. Carlberg, J. Carlsson, "About Random LOS in Rician Fading Channels for MIMO OTA Tests," presented at the 2011 International Symposium on Antennas and Propagation (ISAP 2011), October 2011.
- U. Carlberg, J. Carlsson, **A. Hussain**, P. Kildal, "Ray based Multipath Simulation Tool for Studying Convergence and Estimating Ergodic Capacity and Diversity Gain for Antennas with Given Far-Field Functions," presented at 20th International Conference on Applied Electromagnetics and Communications (ICECom), September 2010.
- **A. Hussain**, P. Kildal, G. Durisi, "Modeling System Throughput of Single and Multi-port Wireless LTE Devices," presented at the IEEE Antennas and Propagation Society International Symposium (IEEE-APS), July 2012.
- X. Chen, P. Kildal, **A. Hussain**, J. Carlsson, "Overview of State-of-the-Art OTA Measurements of Wireless Devices in Reverberation Chamber," will be presented at

International Symposium on Electromagnetic Compatibility (EMC Europe), September 2014.

- **A. Hussain** and P. Kildal, "Estimating TIS of 4G LTE Devices from OTA Throughput Measurements in Reverberation Chamber," will be presented at the IEEE International Conference on Antenna Measurements & Applications (IEEE-CAMA), November 2014.
- P. Kildal, **A. Hussain**, G. Durisi, C. Orlenius, A. Skårbratt, "LTE MIMO Multiplexing Performance Measured in Reverberation Chamber and Accurate Simple Theory," presented at the 6th European Conference on Antennas and Propagation (EuCAP), April 2012.
- B. Einarsson, **A. Hussain**, P. Kildal, "Measurements of Throughput in Reverberation Chamber using Universal Software Radio Peripheral," presented at the 8th European Conference on Antennas and Propagation (EuCAP), April 2014.
- **A. Hussain**, P. Kildal, A. Al-Rawi, J. Yang, "Efficiency, Correlation, and Diversity Gain of UWB Multiport Self-Grounded Bow-Tie Antenna in Rich Isotropic Multipath Environment," presented at the International Workshop on Antenna Technology (IWAT), March 2013.
- H. Raza, J. Yang, **A. Hussain**, "Measurement of Radiation Efficiency of Multiport Antennas With Feeding Network Corrections," IEEE Antennas and Wireless Propagation Letters (IEEE-AWPL), vol. 11, pp. 89-92, January 2012.
- **A. Hussain**, "Interactive Computer Simulation Tools for Effective Teaching and Learning Environments," presented at Chalmers Conference on Teaching and Learning, (KUL 2011), January 2011.

Contents

Abstract	i
Preface	iii
Acknowledgements	v
List of Papers	vii
Contents	xi
List of Acronyms	xiii

Part I: Introductory Chapters

1. Introduction	1
2. Multipath Environment	7
3. 3D-Random Pure-LOS.....	11
4. Model for Throughput of Wireless Devices	15
5. New Method for Measuring Receiver Sensitivity	21
6. Software Defined Radios for MIMO OTA Testing	27
7. Characterization of Multiport Mobile Terminals.....	33
8. Characterization of UWB Bow-Tie Antenna	37
9. Simulation Tools	41
10. Conclusion & Future Work.....	45
Bibliography	47

Part II: Publications

List of Acronyms

2D	Two dimensional
2G	Second Generation
3D	Three dimensional
3G	Third Generation
3GPP	Third Generation Partnership Project
4G	Fourth Generation
ADG	Apparent Diversity Gain
AoA	Angle-of-Arrival
ADC	Analog to Digital Converter
AUT	Antenna Under Test
AWGN	Additive White Gaussian Noise
BLER	Block Error Rate
CDF	Cumulative Distributed Function
CCDF	Complementary Cumulative Distributed Function
DAC	Digital to Analog Converter
DUT	Device Under Test
GSM	Global System for Mobile
GUI	Graphical User Interface
LHS	Left Hand Side
LOS	Line Of Sight
LTE	Long Term Evolution
MED	Mean Effective Directivity
MEG	Mean Effective Gain
MIMO	Multiple Input Multiple Output
MISO	Multiple Input Single Output
MRC	Maximal Ratio Combining
NI	National Instruments
NLOS	Non Line Of Sight
OFDM	Orthogonal Frequency Division Multiplexing
OTA	Over The Air
PER	Packet Error Rate
PSA	Power Spectrum Analyzer
RF	Radio Frequency
RHS	Right Hand Side
RIMP	Rich Isotropic Multipath
SC	Selection Combining
SDR	Software Defined Radio
SIMO	Single Input Multiple Output
SISO	Single Input Single Output
SNR	Signal to Noise Ratio

TIS	Total Isotropic Sensitivity
TRP	Total Radiated Power
USRP	Universal Software Radio Peripheral
UWB	Ultra Wideband
ViRM Lab	Visual Random Multipath Laboratory
VNA	Vector Network Analyzer
WCDMA	Wideband Code Division Multiple Access

Part I
Introductory Chapters

CHAPTER Introduction

1

Traditionally, antennas were widely used for line-of-sight (LOS) communication in different civilian and military applications like radios, TV transmissions, satellite communications, microwave links, radars, etc. A number of research studies were carried out especially to develop methods to measure the performance of these LOS antennas. As a result, the anechoic chamber was developed as a tool to measure LOS antennas and wireless devices. As shown in Fig. 1.1, it has absorbing material on all surfaces (i.e. walls, floor, and ceiling) to emulate the free-space or ideal LOS environment. Many years later, handheld devices such as mobile phones became very popular. These devices are most often present in a non-line-of-sight (NLOS) or multipath environment. Therefore, different methods were developed to measure performance of antennas used in these devices. Today, there is a variety of measurement tools for characterizing over-the-air (OTA) performance of wireless mobile terminals and small antennas in multipath environments. The reverberation chamber is our favorite tool for OTA measurements due to its small size, efficiency, price, and better accuracy. As shown in Fig. 1.2, it is a metallic cavity which emulates rich isotropic multipath (RIMP) environment [1, 2]. The comparison of anechoic and reverberation chambers can be studied from [3-6]. The performance of Multiple-input Multiple-output (MIMO) antenna systems and mobile terminals can be measured inside the reverberation chamber. The measurements show the same improvement in performance as that from theory, e.g. due to antenna diversity in a MIMO system [7].

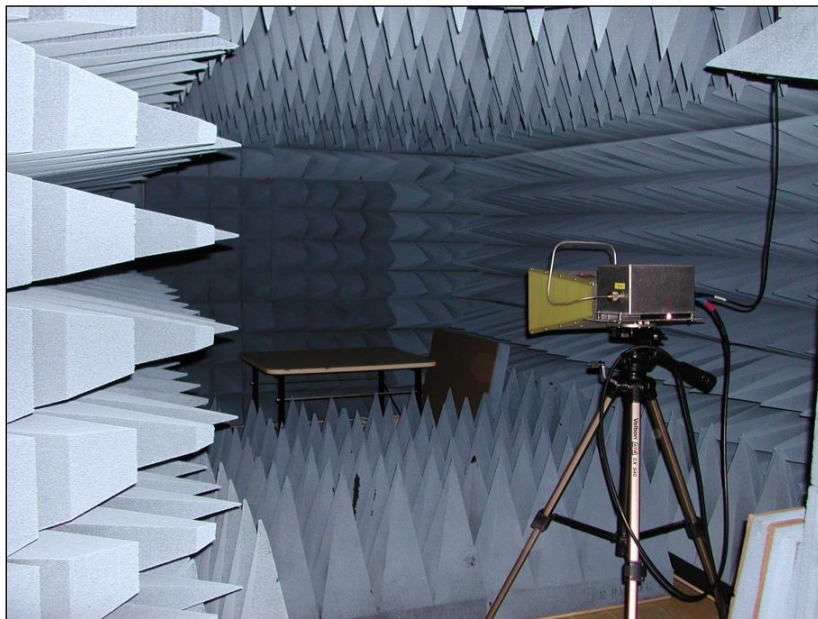


Figure 1.1. Anechoic chamber – a large room with absorbing material on all surfaces.



Figure 1.2. Reverberation chamber – a small metallic cavity with moving stirrers.

Today, it is common to measure OTA performance of both passive (e.g. antennas) and active devices (e.g. mobile terminals) inside a reverberation chamber. This helps us to compare antenna performance as well as complete system performance. For example, it has been used to measure radiation efficiency, correlation, diversity gain, and capacity of MIMO antennas [7-10], sensitivity of RFID tags [11], and OTA throughput of MIMO LTE systems [12-16]. Fig. 1.3 shows a LTE device inside a reverberation chamber during MIMO OTA measurements. Further details on LTE throughput measurements and simulations are presented in Chapter 4.



Figure 1.3. Huawei E398 LTE USB modem connected to two external antennas inside reverberation chamber during MIMO OTA throughput measurements.

The measurement accuracy of the reverberation chamber studied in [17-24] shows that it performs very well with a standard deviation within ± 0.5 dB. The environment inside the reverberation chamber is controlled in terms of coherence bandwidth [25-27]. Furthermore, it

has been shown that the measurements performed inside the reverberation chamber are repeatable. Some recent examples of passive and active measurements inside reverberation chamber can be found in [7, 16].

The LTE throughput measurements inside reverberation chamber are performed for a commercially available LTE device, e.g. Huawei E398 LTE USB modem. It is important to be able to measure the performance of LTE wireless devices and to be able to identify good and bad devices. However, it is difficult to get full control over the device and to get detailed information about it. To overcome this situation and get more control over hardware and software, we used a Software Defined Radio (SDR). Today, the most extensively used SDR is called Universal Software Radio Peripheral (USRP). It is developed by Ettus Research and its parent company National Instruments (NI). Fig. 1.4 shows USRPs during a conducted throughput measurement.

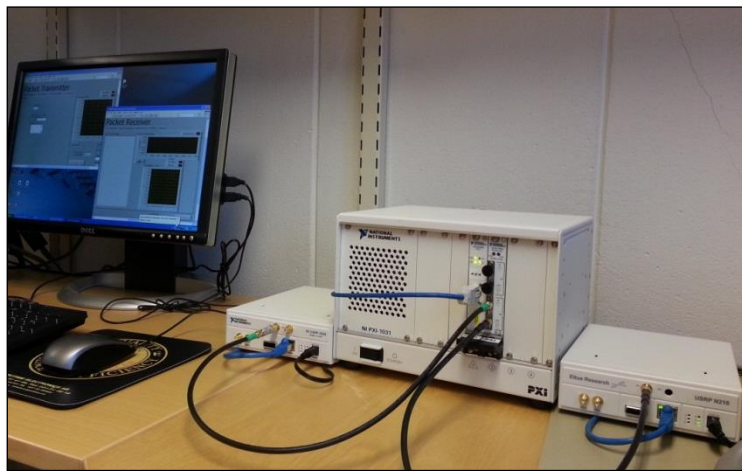


Figure 1.4. USRPs connected via digital attenuator during conducted throughput measurements.

Both USRPs and the attenuator are controlled via LabVIEW program on the computer.

USRPs allow us freedom to design a communication system in LabVIEW and enable us to accurately test different scenarios e.g. OTA throughput with inverse power allocation, diversity combination schemes, etc. Therefore, it is easier to evaluate, compare, and model system performance since we have all information we need and control over every single bit. To the best of our knowledge, we are the first to evaluate the OTA performance of USRPs using reverberation chamber. The measurement and simulation results are presented in Chapter 6.

The latest LTE mobile phones are equipped with multiport antennas. The measurements and simulations of a multiport mobile phone mockup in RIMP have shown good agreement in [28]. The simulations use far-field patterns to calculate the diversity gains for different standard talk positions on both sides of the head as defined in [29]. A practical mobile phone mockup together with the head and hand phantom taken from examples in CST Microwave Studio is shown in Fig. 1.5.

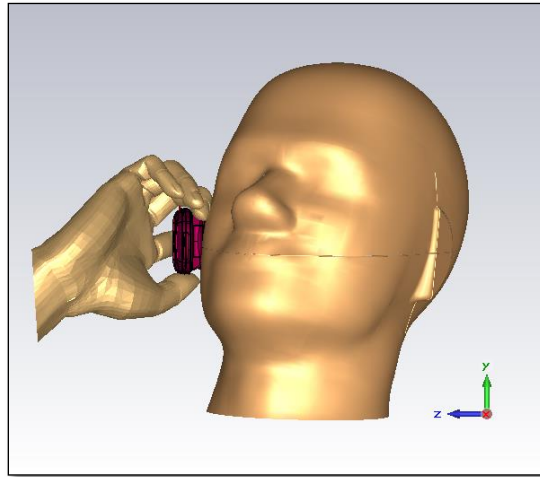


Figure 1.5. A practical mobile handset model together with head and hand phantom taken from examples in CST Microwave Studio.

While fixed antenna systems are being measured in anechoic chamber (emulating free-space environment) and mobile terminals are being measured in reverberation chamber (emulating multipath environment), there still exist real-life situations when mobile terminals experience a LOS component in a multipath environment. The randomness due to user is very important but has often been ignored. We argue that LOS experienced by a mobile terminal will become completely random due to random position and orientation of the terminal with respect to the nearest base station [1, 30]. We use the terminology “random LOS” to express a pure LOS which, due to the user, becomes random in three-dimensional space i.e. 3D-random. The OTA performance of wireless devices with random position and orientation in the two extreme environments i.e. random LOS and RIMP is studied in this thesis. Our hypothesis is:

“If the performance of device is good in both extreme environments i.e. RIMP and pure-LOS, then its performance will be good in real-life environments as well.” [31]

The OTA performance of a MIMO antenna system depends mainly on its total embedded radiation efficiency and the correlation between the antenna ports in RIMP while spatial coverage and polarization diversity are the two additional key factors that determine the OTA performance in random LOS. This means that the MIMO antenna system with high radiation efficiency, low correlation, isotropic antenna pattern, and dual polarization is the ideal antenna which will perform best in both extreme environments i.e. RIMP and random LOS.

Recent progress at our research group has led to the development of an ultra-wideband (UWB) self-grounded bow-tie antenna [32-35]. The OTA performance of this UWB MIMO antenna is studied in RIMP and in random LOS. Due to its wide bandwidth, high efficiency, and compact size it has attracted a lot of applications. Today, it is also used as a multiport base station antenna for reverberation chambers by Bluetest AB. The performance of this antenna is presented in Chapter 8.

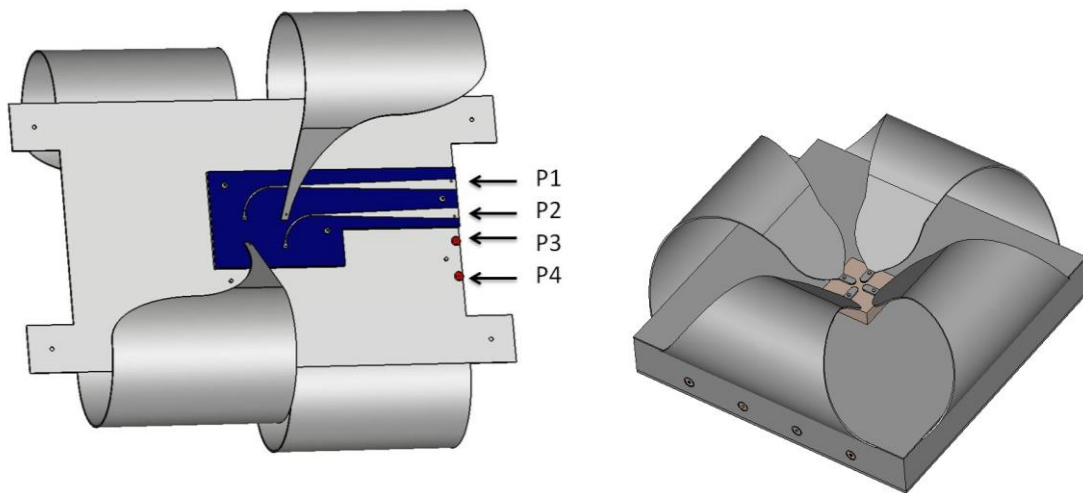


Figure 1.6. Graphical models of two different versions of four-port UWB self-grounded bow-tie antenna.

At Chalmers University, we have also developed numerical tools to simulate channel models and estimate OTA performance of small antennas and wireless terminals. Examples of such simulation tools are: (i) Rayleigh-lab [36] which is based on random number generator, and (ii) ViRM-lab [37] which is a ray-based simulation tool. These tools are open source and were initially developed to study convergence of radiation efficiency, diversity gain, and MIMO capacity in RIMP. After some years of development in the code, now we can also study random LOS and MIMO performance. Rayleigh-lab and ViRM-lab are further discussed in Chapter 9.

CHAPTER Multipath Environment

2

A multipath environment is simply an environment in which the signal from one antenna takes multiple paths to arrive at another antenna. The signal experiences different phenomena such as reflection, refraction, diffraction, interference, and scattering in the environment due to multipath propagation. The signals in a multipath environment interfere constructively and destructively. The peaks in the received fading signal appear due to constructive interferences and deep nulls appear due to destructive interferences. Due to different propagation effects, the received signal amplitude, phase, and polarization become random. Mobile terminals, e.g. tablet computers, mobile phones, etc., undergo strong fading in multipath environments such as urban and indoor environments. The instantaneous fading of the signal is completely random for different frequency, space, time and polarization. Different techniques such as diversity in frequency, space, time, or polarization can be used to overcome deep fading nulls and improve the performance of the mobile terminals in multipath environments. A multipath environment is usually characterized by the distribution of the fading signal e.g. Rayleigh fading, Rician fading, etc.; delay spread or coherence bandwidth; coherence time or Doppler spread; number of scatterers; position and distribution of scatterers; polarization imbalance.

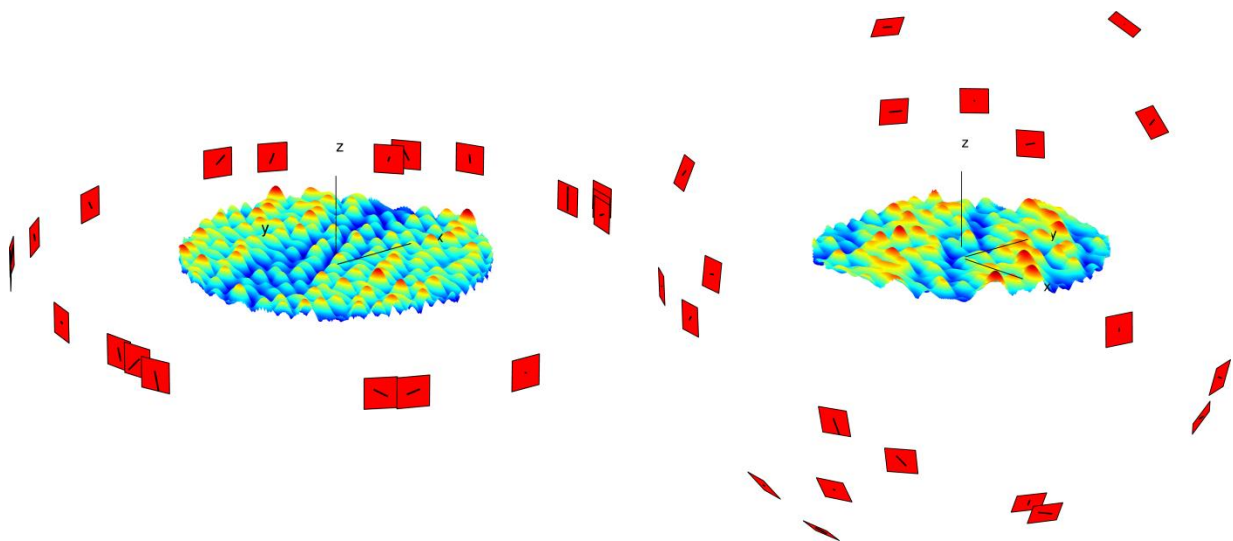


Figure 2.1. Illustration showing incoming waves with random angle-of-arrival, polarization angle, amplitude and phase in 2D (left) and 3D (right) multipath environments.

Several groups such as 3GPP, CTIA, COST, etc. have proposed different models for propagation in multipath environments. Often it becomes a point of discussion if the multipath environment model should be 2D or 3D, as shown in Fig. 2.1. It is argued in some studies that in real-life multipath environments the waves are mostly in the horizontal plane forming a 2D multipath environment. We use ray-based multipath simulation tool called ViRM-lab, and show that measurements performed in a 2D multipath environment will depend on the position and orientation of the mobile terminal [2, 37]. Different positions and orientations in a 2D multipath environment will give different results. On the other hand, in a 3D multipath environment the results are always unique and do not depend on the position and the orientation of the terminal. A comparison of simulated apparent diversity gain (ADG) performance of two dipoles in 2D and 3D multipath environments is presented in [2], also shown in Fig. 2.2. The channels on all antenna ports are combined using selection combining (SC) scheme to calculate ADG.

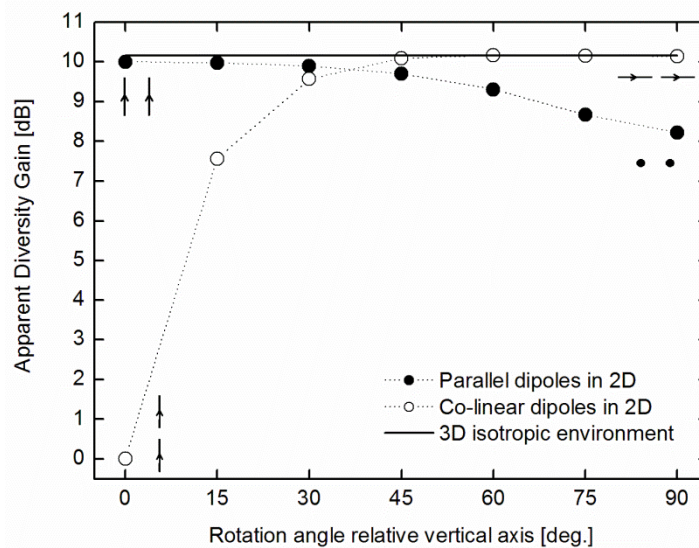


Figure 2.2. Apparent diversity gains of two parallel and co-linear dipoles in 2D and 3D multipath environments.

The reverberation chamber is a metallic cavity and has stirrers to stir the energy by mechanical movement of the plates inside the chamber as shown in Figs. 1.2 and 2.4. The device-under-test (DUT), e.g. laptop, lies on the platform stirrer which rotates the DUT inside the multipath environment. The long metal sheet between the transmit antenna and the DUT is to block LOS-component for better accuracy in the measurement results. The reverberation chamber emulates rich isotropic multipath (RIMP) environment [1]. The angle-of-arrival (AoA), phase, and polarization angle of these incoming waves are uniformly distributed. The received complex voltages at the antenna ports are complex Gaussian distributed. The reverberation chamber has been used for measuring active and passive devices in RIMP environment for more than 10 years. The antenna radiation efficiency, correlation, and diversity gain are examples of passive measurements while the total radiated power, total isotropic sensitivity, and throughput are examples of active measurements inside reverberation chamber.

The measurement and simulation for OTA characterization of an antenna or a DUT in RIMP environment are independent of the shape of its radiation pattern, and its position and

orientation in the environment. The cumulative distribution function (CDF) of the received voltages at the antenna port with 100% antenna efficiency always follows Rayleigh distribution in RIMP environment for omnidirectional and directional antennas. This shows that the measurements in RIMP environment are independent of the shape of the far-field radiation patterns. A comparison of two incremental electric dipoles and two pencil beams in RIMP environment is shown in Fig 2.3 in terms of diversity gain performance and Shannon's channel capacity. The pencil beams with -3 dB half beamwidth of 45 degrees are used. From the results in Figs. 2.2 and 2.3, it is clear that the diversity gain and channel capacity converge to a unique value in a 3D multipath environment independent of the position and orientation of the device, and the shape of its far-field radiation patterns.

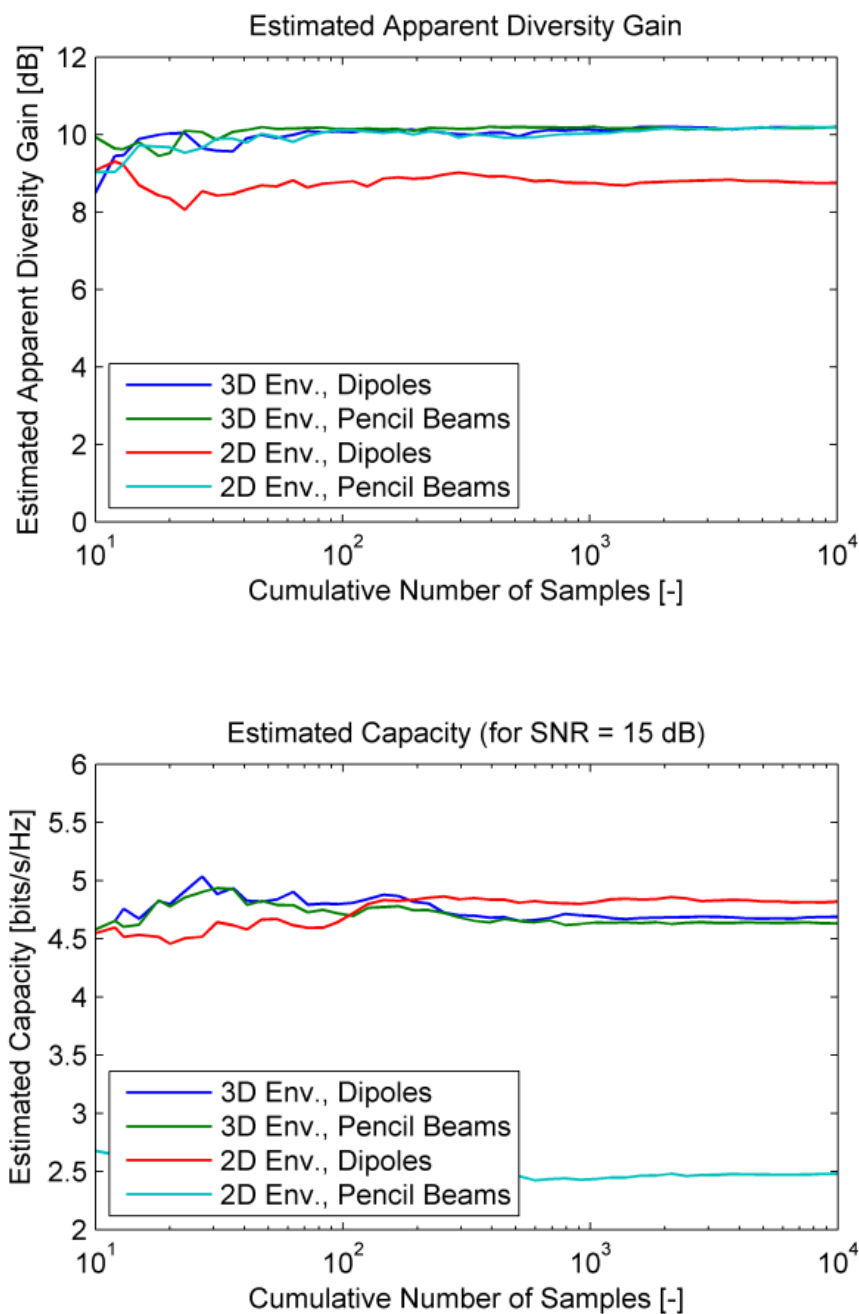


Figure 2.3. Apparent diversity gain (top) and Shannon's channel capacity (bottom) of two dipoles and two pencil beams in 3D and 2D multipath environments.

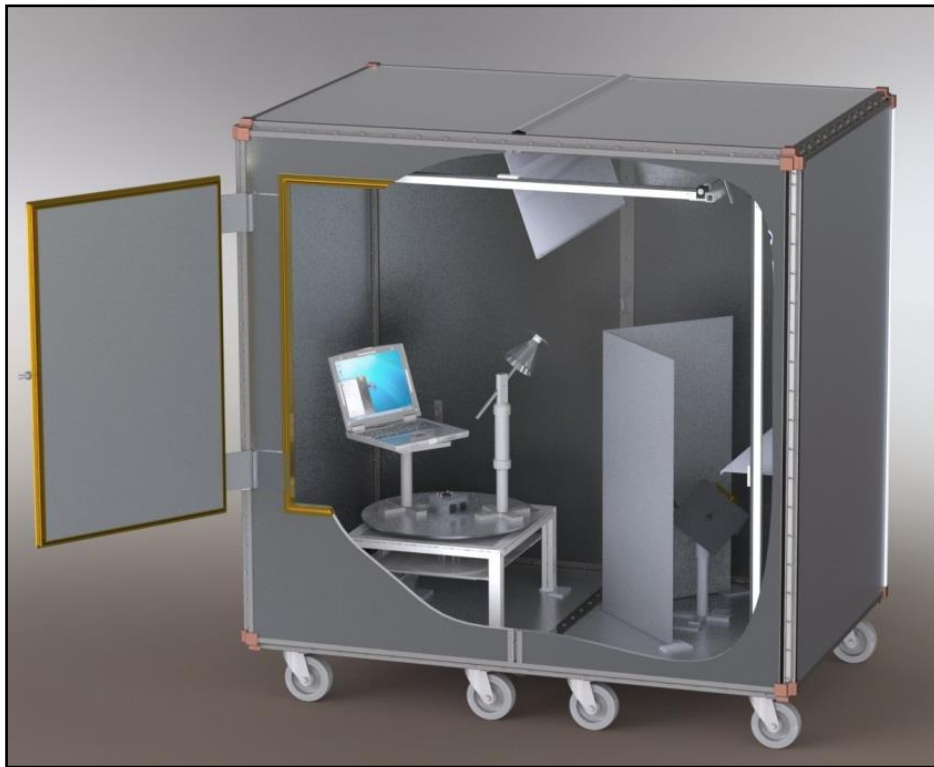


Figure 2.4. A drawing of an interior view of reverberation chamber (one wall is partly removed) with plate stirrers and a rotating platform stirrer carrying the device-under-test.

CHAPTER 3D-Random Pure-LOS

3

Traditionally, the LOS channel is known as a fixed and deterministic channel because the environment between the two LOS antennas does not change e.g. microwave links, TV transmission, satellite communication, etc. As a consequence, the phase, amplitude, and polarization are fixed for the LOS antenna system. In contrast to LOS channel, the mobile terminals experience a NLOS channel or multipath which is neither fixed nor deterministic; it is varying randomly in all dimensions, i.e. space, frequency, time, and polarization. The mobile terminals are mostly used indoors, e.g. home, office, shopping center, etc., where there are many moving and scattering objects around the mobile terminal.

Although the mobile terminals are most often present in scattering environments yet there are situations in which these mobile terminals are present in pure-LOS e.g. mobile terminals very close to the micro base station in a non-scattering environment. Now we question ourselves if this pure-LOS channel looks like the traditional LOS channel which is fixed and deterministic. Yes, it is a fixed and deterministic LOS channel provided that the position and orientation of the terminal is fixed. In reality, the user is random in position and orientation and therefore the mobile terminal. If we assume that the mobile terminal has a random position and orientation in a three dimensional space, then the pure-LOS channel will appear as a 3D-random pure-LOS channel at the antenna port of mobile terminal. We simulate the 3D-random pure-LOS model by using a single incoming LOS wave with fixed amplitude, uniformly distributed phase, angle-of-arrival, and polarization angle. The randomness in the LOS-component of the channel has been presented for diversity gains in [1]; for capacity of mobile multiple-antenna wireless link in [38]; for MIMO OTA-tests in Rician fading in [39].

From the illustration of random orientation of Huygen's source in pure-LOS in Fig. 3.1, it is easier to understand the 3D-random pure-LOS channel model due to the randomness of the user. The random position of the terminal makes the phase of the incoming wave appear random. The random orientation of the terminal makes the angle-of-arrival of the incoming wave and the polarization-angle appear random at the antenna port of the mobile terminal.

The simulated results in random-LOS are presented in Fig. 3.2 that show CDFs of the received voltages at each port of the antenna on a mobile phone mockup and its MRC-combined diversity channel [40]. Originally, the diversity gain was defined for a single user in a RIMP environment, typically at 1% CDF level. Recently, the diversity gain is defined for a bunch of users with 3D-random orientation and position of the mobile terminal, i.e. in random-LOS [1], typically for 1% users with worst performance. For measuring the diversity gain in random-LOS, we introduce a new unit dBR i.e. difference of power-levels in dB relative to ideal Rayleigh. From the results in [40], it can be observed that antennas with regular shape far-field patterns, e.g. dipole antennas, in

random-LOS do not follow ideal Rayleigh distribution. Far-field patterns are irregular in shape in real-life scenario due to the effect of chassis, user head, hand, and body, and therefore will more likely follow the Rayleigh distribution.

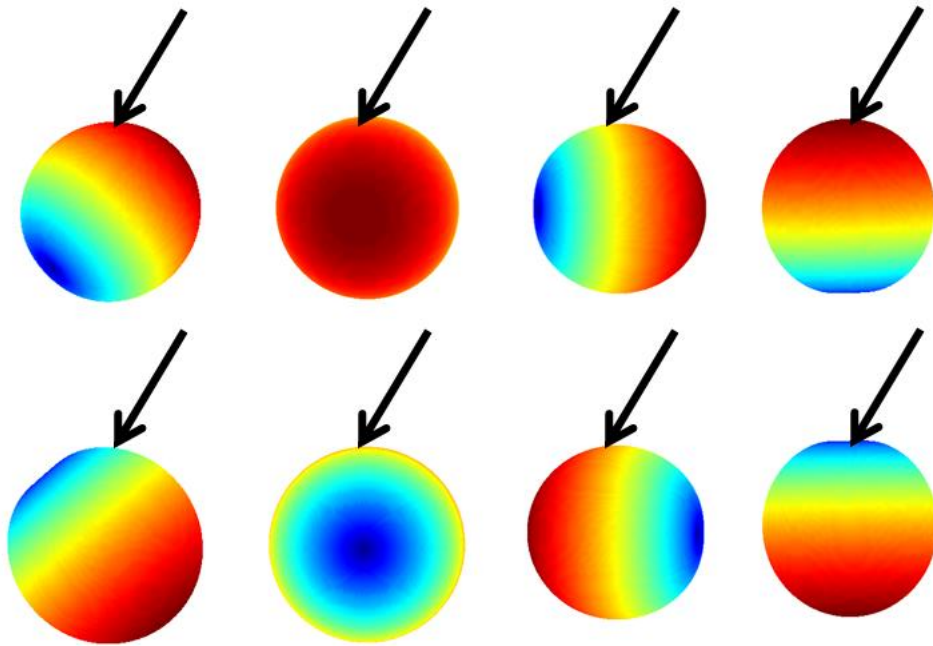


Figure 3.1. Illustration of random orientation of the Huygen's source in the presence of LOS.

From illustration in Fig. 3.3, it is shown that the orientation of the phone is not fixed. When a user holds a phone on the right side of the head, the marked arrow is in a horizontal direction. The direction of this arrow becomes vertical when the user holds the phone on the left side of the head. The LOS-component is fixed but appears random due to the random orientation of the terminal.

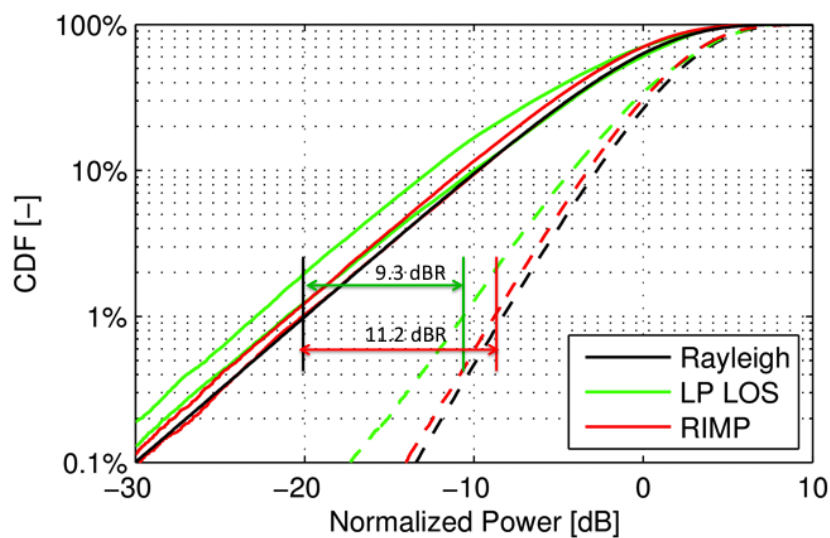


Figure 3.2. CDFs of two-port antenna on a phone mockup in RIMP and random-LOS with linearly polarized (LP) incoming waves.

The diversity gain in 3D-random pure-LOS is defined in terms of dBR i.e. diversity gain with reference to ideal Rayleigh CDF, typically defined at 1% CDF-level. This is shown in Fig. 3.2.

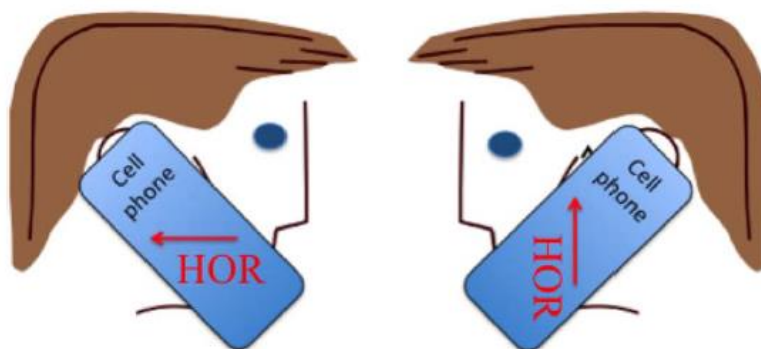


Figure 3.3. A user holding a phone with a marked arrow on right side (left) and left side (right) of the head shows that the direction of arrow changes from horizontal to vertical respectively.

The study of random pure-LOS can be extended in future e.g. by studying diversity gain and throughput for LTE MIMO terminals.

CHAPTER

4

Model for Throughput of Wireless Devices

Today LTE is one of the latest telecommunication standards for mobile phones after its predecessors GSM and WCDMA. The main advantage of using LTE is higher throughput by contributions from MIMO and OFDM diversity gains. The flexibility to choose modulation scheme, bandwidth, block size, code rate, MIMO-multiplexing or MIMO-diversity has made the system quite robust to adjust to the environment in different Signal-to-Noise Ratio (SNR) regimes. On the other hand, this makes the system design more complicated. In this chapter, a simple theoretical model based on a threshold receiver model for simulating the OTA throughput performance of LTE devices is presented. The model has been tested on a commercially available LTE device and the simulated results are in good agreement with the measurements performed in a reverberation chamber [15].

The proposed model is very simple and includes the effect of spatial-diversity (MIMO) and frequency diversity (OFDM). The model is shown in (4.1) below:

$$T = R \times CCDF(P_t/P_{av}) \quad (4.1)$$

$$CCDF(P_t/P_{av}) = 1 - CDF(P_t/P_{av}) \quad (4.2)$$

$$CDF(P_t/P_{av}) = \int_0^{P_t} pdf(P/P_{av}) dP \quad (4.3)$$

Here, T is throughput, R is maximum achievable data-rate, P_t is threshold power, P_{av} is average signal power received by the terminal, P is received signal power, pdf is probability density function, CDF is cumulative distribution function, and $CCDF$ stands for complementary CDF .

In our study, the threshold power P_t is always a measured quantity and it is fixed for a given combination of system configuration and receiver terminal. It is measured in an Additive White Gaussian Noise (AWGN) channel (i.e. no fading) by connecting a cable directly between the external antenna-port of the LTE terminal and the LTE base-station. The measurement setup is illustrated in Fig. 4.1.

To use (4.1) for estimating the OTA-throughput of an LTE device, we need to calculate the $CCDF$ of the MRC-combined diversity channel, which includes spatial diversity due to MIMO and frequency diversity due to OFDM. The total number of channels to compute the $CCDF$ of the diversity channel is known simply by multiplying number of frequency diversity channels

N_{fd} , number of transmit antennas N_t , and number of receive antennas N_r as shown in (4.4). The number of frequency diversity channels N_{fd} is calculated simply by taking the ratio of system bandwidth and coherence bandwidth as shown in (4.5).

$$N_{total} = N_{fd} \times N_t \times N_r \quad (4.4)$$

$$N_{fd} = B_s/B_c \quad (4.5)$$

The larger the coherence bandwidth B_c , the smaller will the frequency diversity N_{fd} be for a given system bandwidth B_s and vice versa. Similarly, the larger the system bandwidth B_s , the larger will the frequency diversity N_{fd} be. But larger system bandwidths B_s require higher SNR to support higher data-rates.

The measurement setups for both conducted measurements and OTA measurements are shown in Fig. 4.1 below:

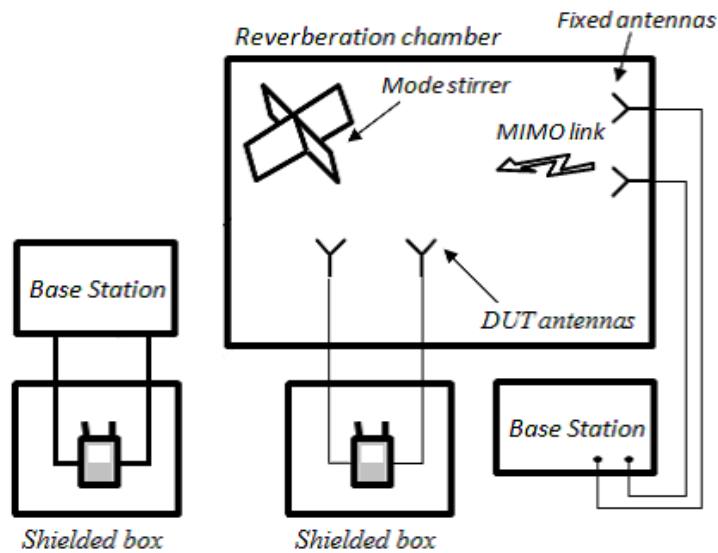


Figure 4.1. Conducted measurement setup (left) and OTA measurement setup (right)

The model has been tested for both different coherence bandwidths and different system bandwidths in [16], also shown in Fig. 4.2. The coherence bandwidth of the channel inside reverberation chamber is controlled by lossy objects inside the reverberation chamber. The relationship between coherence bandwidth B_c and delay spread σ inside reverberation chamber is shown below [26]:

$$B_c = \sqrt{3}/\pi\sigma \quad (4.6)$$

In Fig. 4.2 we can see that the OTA throughput is increasing with the increasing average power. Also, the slope of the throughput curves (representing the frequency diversity) is different for different coherence bandwidths B_c for a given system bandwidth B_s . The results show LTE

throughput of 2×2 MIMO using transmit-diversity for fixed 64-QAM modulation scheme. In reality, the modulation scheme is adaptable and not fixed. Higher modulation schemes such as 64-QAM and 128-QAM are supported at higher power levels, and lower modulation schemes such as 16-QAM and 4-QAM are supported at lower power levels. At the time of writing this thesis, there is no commercial LTE base station simulator available which can provide adaptive modulation schemes.

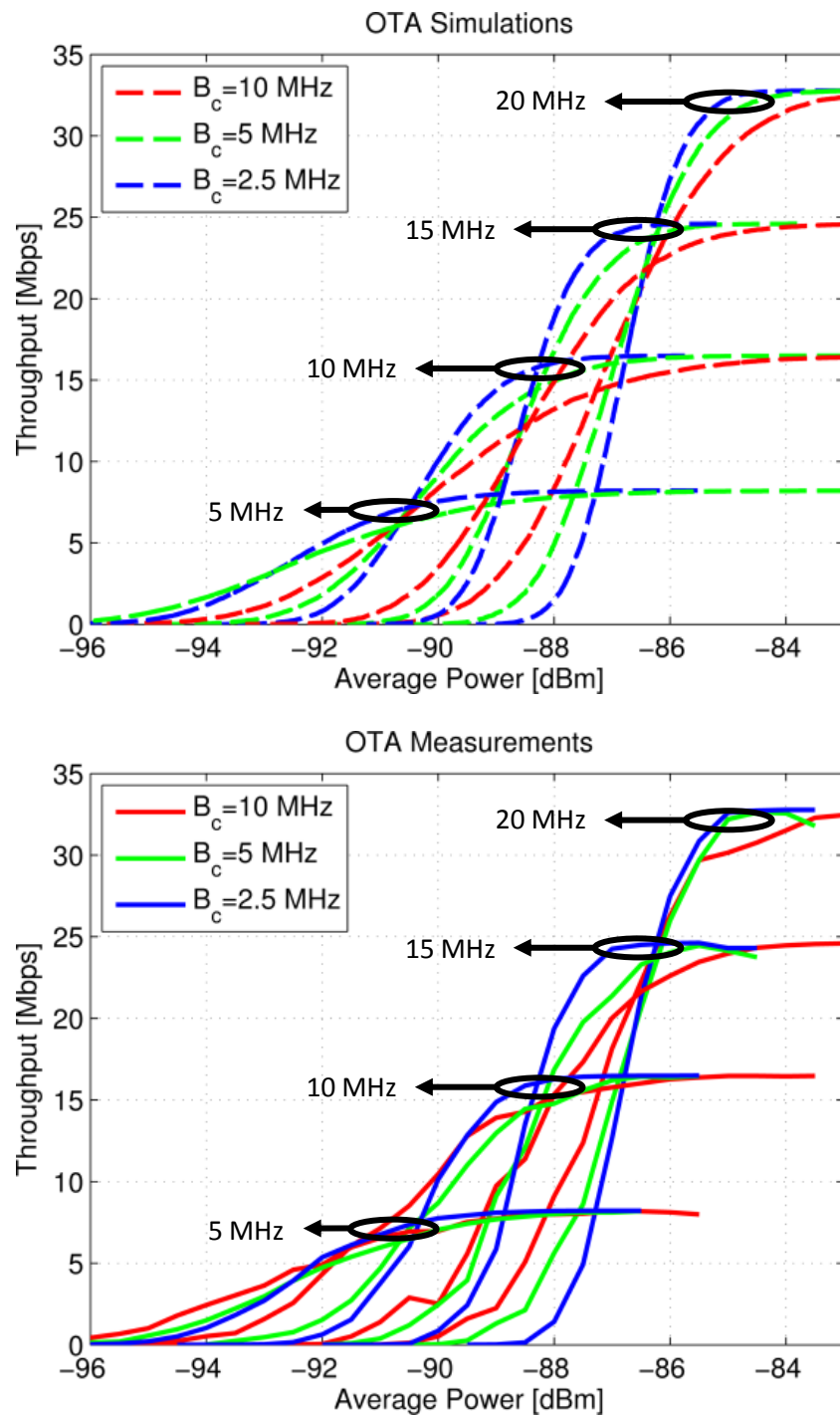


Figure 4.2. OTA-simulations (top) and -measurements (bottom) of 2×2 MIMO LTE throughput for system bandwidths of 20, 15, 10, and 5 MHz; coherence bandwidths of 10, 5, and 2.5 MHz.

The proposed model for estimating throughput in (4.1) shows the relationship between CDF and throughput. This relationship can be seen in Fig. 4.3, i.e. diversity gain at 1% CDF-level is the same as the diversity gain at 99% throughput-level.

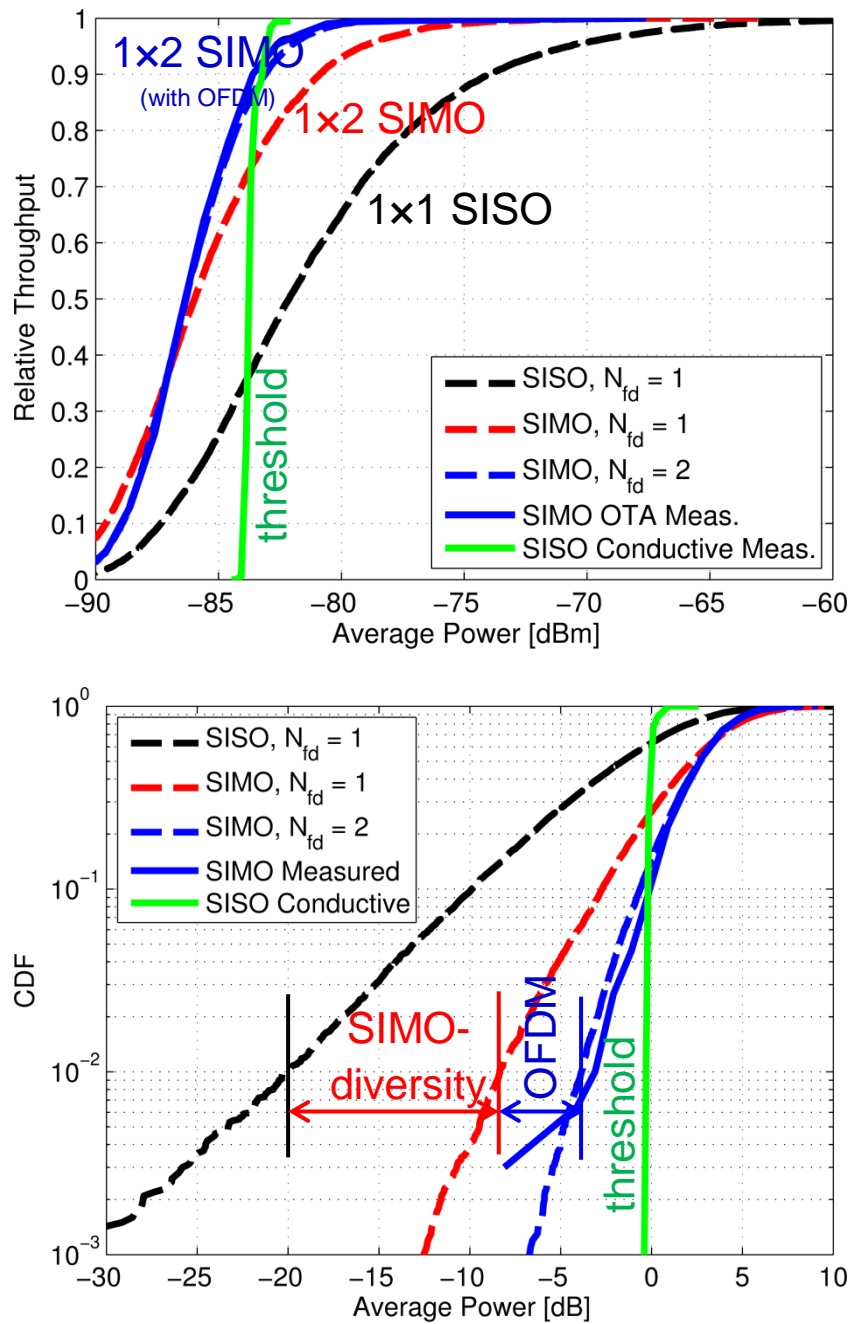


Figure 4.3. Theoretical (dashed) and measured (solid) lines for relative throughput (upper) and corresponding CDFs (lower) for LTE device with two-port MIMO antenna. $P_t = -83.7$ dBm.

Similarly, we can model LTE throughput of 2×2 MIMO system when each transmit antenna is transmitting a different data-stream i.e. multiplexing as shown in [13]. An illustration of a digital receiver block diagram in 2×2 MIMO-multiplexing configuration is shown in Fig. 4.4. When MIMO is used in spatial multiplexing configuration, parallel data streams can be transmitted over the wireless fading channel. Interference between the data streams can be removed using suitable pre-processing and post-processing techniques.

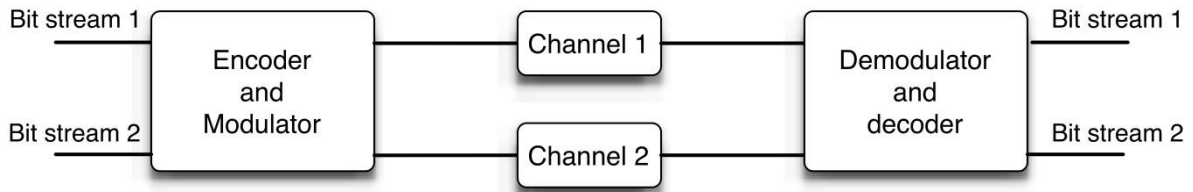


Figure 4.4. Digital receiver block diagram of a 2×2 MIMO system operating in spatial multiplexing configuration.

The throughput in the MIMO-multiplexing case is doubled because R the maximum achievable data-rate is now doubled compared to the MIMO transmit-diversity case. Since we use two receiver chains, the average of the threshold powers of the receivers P_{tav} will be used as shown below:

$$P_{tav} = \frac{P_{t1} + P_{t2}}{2} = \frac{P_t}{2} \left(\frac{1}{e_1} + \frac{1}{e_2} \right) = \frac{P_t}{2} \left(\frac{e_1 + e_2}{e_1 e_2} \right) \quad (4.7)$$

We have assumed here that both receivers in the MIMO device are the same and their threshold powers P_{t1} and P_{t2} can only vary due to their antenna efficiencies e_1 and e_2 . In reality there can be devices which have receivers with dissimilar performances due to differences in the system design and implementation. We leave these complexities for further studies and use our simple formula for estimating throughput of wireless devices which includes the gains due to spatial diversity as well as frequency diversity.

CHAPTER

5

New Method for Measuring Receiver Sensitivity

The total isotropic sensitivity (TIS) is one of the most significant OTA measure for the evaluation of the receiver quality of wireless devices often mentioned in the specifications of wireless electronic devices such as mobile phones, WiFi routers, and 4G modems. The TIS is a measure of the average sensitivity of a complete communication system including receiver sensitivity, antenna efficiency, and noise, when the averaging is performed over the complete 3-dimensional sphere. The sensitivity of the receiver is the minimum required signal strength at which the receiver will work in an ideal LOS channel or AWGN. Traditionally, the TIS of a DUT has been measured in anechoic chambers but today it is also measured in reverberation chambers. The introduction of 4G LTE standards brings improvement in the TIS of a system by spatial diversity and multiplexing gains due to MIMO and frequency diversity gain due to OFDM. The TIS measurements are extremely time consuming, and do not show the effect of frequency diversity. On the other hand, the throughput measurements clearly show the effect of diversity due to MIMO and OFDM. The measurement setup for both TIS and throughput is the same, see Fig. 5.1; however, the measurement procedure is different. The TIS and throughput measurement procedures are explained in detail in the attached paper [B3].



Figure 5.1. A measurement setup for total isotropic sensitivity and throughput measurements. An LTE base station is connected to a reverberation chamber using cables. The DUT is inside the reverberation chamber and connected to external antennas.

For a given antenna configuration and given settings such as frequency, modulation and coding schemes, and bandwidth the receiver sensitivity of a DUT is fixed. Furthermore, the receiver

sensitivity is dependent on the performance of the receiver hardware components as well as the signal processing algorithms built into the DUT. We have shown that for an ideal SISO system with 100% antenna radiation efficiency e_{rad} and no noise coupling, the TIS is equal to the receiver threshold power P_{th} . Mathematically, this can be expressed as:

$$P_{TIS} = \frac{P_{th}}{e_{rad}} \quad (5.1)$$

The derivation of (5.1) is given in paper [B3]. We will show using Figs. 5.2 and 5.3 that our method can estimate TIS for all antenna system configurations i.e. both SISO and MIMO, and also for cases where there is frequency diversity due to OFDM.

Figure 5.2 shows results from a simulation of a SISO system without frequency diversity (left figure) and with frequency diversity (right figure). The blue lines represent the thresholds of an ideal threshold receiver due to varying quality of the channel in different static stirrer positions inside the reverberation chamber. For given software and hardware configurations, both the threshold and the sensitivity of the threshold receiver are fixed, so why do we see different thresholds if it is supposed to be fixed? The reason is that the instantaneous path loss is random for each stirrer position and, when doing this investigation, we use the average path loss inside the reverberation chamber. Therefore, it seems that the instantaneous receiver threshold P_{th} (represented by blue lines in Fig. 5.2) is random by changing the stirrer position.

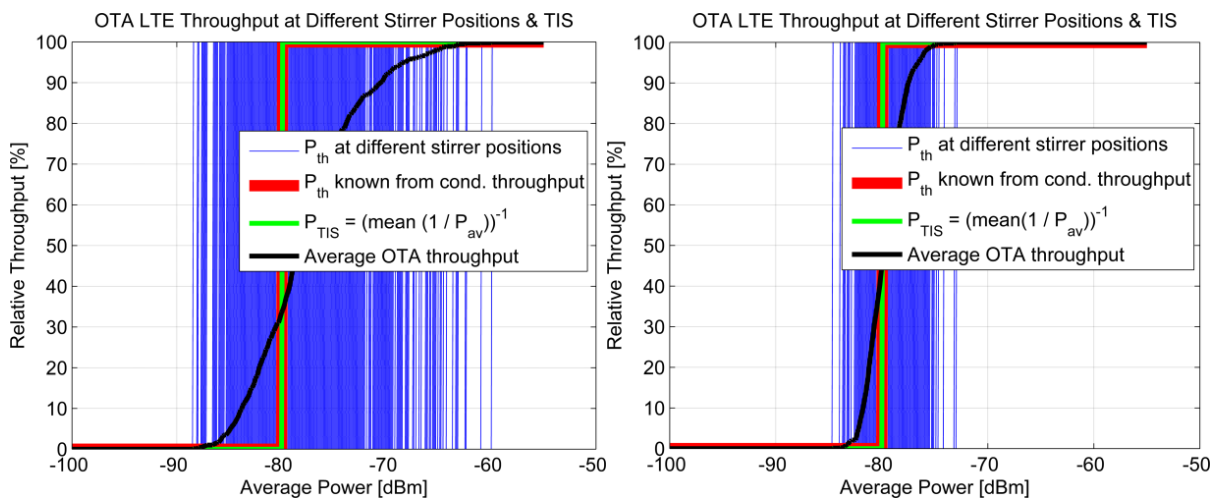


Figure 5.2. The TIS and throughput of a SISO system without frequency diversity (left), and with frequency diversity (right).

We can also reason that the spatial distribution of incoming waves towards the DUT is different in different stirrer positions and therefore the instantaneous P_{th} depends very much on the shape of the radiation pattern. If we use an extreme example of pencil beam antenna in a stirrer position in which none of the incoming waves are in the direction of main beam then the base station will have to increase the average power level P_{av} of the cell to get 100% throughput on an ideal threshold receiver. This example represents a very bad channel condition and as a result the threshold of the receiver will be very high e.g. a blue line at -60 dBm in Fig. 5.2. In other words, the base station has to transmit higher average power in bad channel conditions and vice versa.

The red line in Fig. 5.2 is the threshold of the receiver P_{th} at -80 dBm which is known from conducted throughput measurement of the device. The green line represents the TIS which is also at -80 dBm and calculated by following the formal TIS measurement procedure defined by wireless industry standards. The value of P_{TIS} is calculated by using P_{av} values of all blue lines in Fig. 5.2 when the throughput is 100% and then averaging them using the formula given below [41]:

$$P_{TIS} = \left(\frac{1}{N} \sum_{n=1}^N \frac{1}{P_{av,n}} \right)^{-1} \quad (5.2)$$

Here n is the stirrer position number and N is the total number of stirrer positions. Equation (5.2) is valid under the assumption that the average path loss in the reverberation chamber and the cable losses are calibrated out. The TIS and throughput measurements in the reverberation chamber are independent of the position and the orientation of the DUT. The black curve represents the OTA throughput, which has a smaller slope when there is no OFDM (Fig. 5.2 - left), and a larger slope when there is OFDM (Fig. 5.2 - right).

From Fig. 5.2 it can be concluded that: (a) for an ideal threshold receiver, the TIS of a 1×1 SISO system is the same as P_{th} , (b) the TIS does not depend on the frequency diversity of the system, and (c) the higher the frequency diversity, the closer the OTA throughput is to the threshold of the receiver. Ideally for 1×1 SISO system with a threshold receiver and without frequency diversity, the TIS is equal to the average power level at 36% OTA throughput. OTA throughput and TIS measurements are related to each other because they are both measured using the same measurement setup inside the reverberation chamber, and therefore experience the same multipath environment. Moreover, it makes sense to use the OTA throughput to represent the receiver sensitivity because the throughput is much faster and easier to measure.

In Figs. 5.3 and 5.4, we illustrate the effect of increasing frequency diversity order N_{fd} on the OTA throughput curves for both 1×1 SISO and 2×2 MIMO antenna configurations respectively. We observe that the slope of the OTA throughput curve becomes larger and the throughput curve converges to an ideal threshold-like curve when there is the effect of OFDM. To estimate the TIS from the OTA throughput of SISO and MIMO systems with any frequency diversity order N_{fd} , the corresponding theoretical throughput-level is needed. Table 5.1 gives theoretical throughput levels for a number of SISO and MIMO configurations.

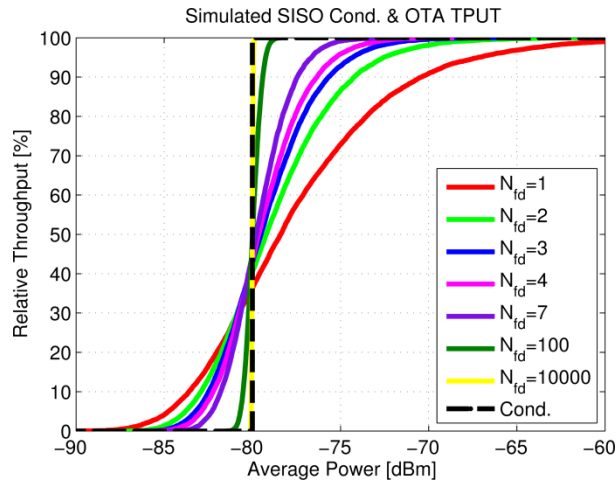


Figure 5.3. OTA throughput curves for 1×1 SISO for increasing orders of frequency diversity.

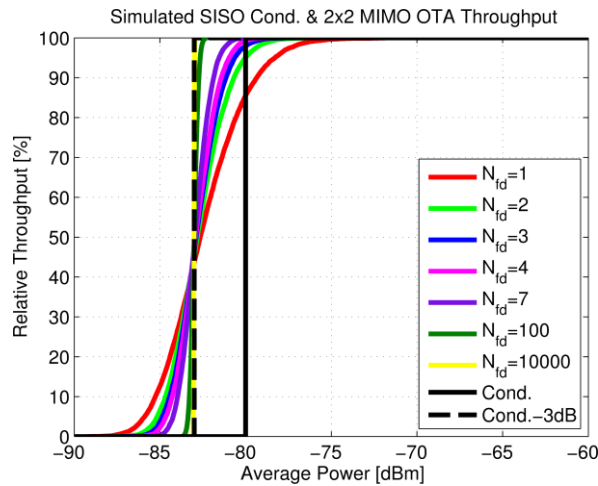


Figure 5.4. OTA throughput curves for 2×2 MIMO for increasing orders of frequency diversity.

The 2×2 MIMO OTA throughput curves converge at -83 dBm, which is 3 dB better than the threshold. Therefore, a -3 dB shifted threshold curve representing TIS is added in Fig. 5.4. Then we find the OTA throughput levels at which TIS can be estimated for 2×2 MIMO systems in different frequency diversity orders. Therefore, we can conclude from Fig. 5.3 that the TIS of an ideal threshold receiver is equal to the threshold for SISO systems only. From here we see that there is a need to generalize (5.1) to describe any $M \times M$ MIMO system. Mathematically, it can be expressed as follows:

$$P_{TIS} = \frac{P_{th}/M}{e_{rad}} \quad (5.3)$$

Equation (5.3) shows that as M increases (i.e. the size of the MIMO system increases), the better will be the TIS of the MIMO system compared to the threshold P_{th} . This is exactly what we see in Fig. 5.3. Note that for an ideal DUT we assume antenna radiation efficiency e_{rad} equal to 100% and no mutual coupling between the antenna ports.

TABLE 5.1. OTA THROUGHPUT (TPUT) LEVEL TO ESTIMATE TIS

N_{fd}	$N_{RX} \times N_{TX}$	<i>OTA TPUT-level to estimate TIS X [%]</i>
1	1×1	36%
2	1×1	40%
3	1×1	43%
4	1×1	43%
7	1×1	45.5%
∞	1×1	0-100%
1	2×2	43.5%
2	2×2	45.2%
3	2×2	46.5%
4	2×2	47.2%
7	2×2	48%
∞	2×2	0-100%

The values in Table 5.1 are obtained using the ideal theoretical throughput curves shown in Figs. 5.3 and 5.4. Comparing SISO and MIMO systems in Figs. 5.3 and 5.4, we also observe that both the OTA throughput curves and the TIS for 2×2 MIMO systems (with transmit and receive diversity) is 3 dB better than for 1×1 SISO systems. The threshold will be fixed in both cases e.g. -80 dBm.

CHAPTER

6

Software Defined Radios for MIMO OTA Testing

During the last decade, software defined radios (SDR) have been developed to serve the wireless industry and academia as a platform for experimentation in various research projects. It is a powerful and inexpensive radio platform where the radio link parameters are defined on software. The SDRs are often used as test beds and enable us to test and compare e.g. different signal processing algorithms, antenna configurations, modulation schemes, etc. In other words, we can characterize different hardware and software components of a radio link. The most popular SDR at the time of writing this thesis is called Universal Software Radio Peripheral (USRP) which is designed and developed by Ettus Research and its parent company National Instruments (NI), see Fig. 6.1. A USRP is a simple general purpose radio platform and can be used for any application. We found it quite useful as an inexpensive instrument for OTA testing of single port and multiport antennas, and MIMO communication systems inside reverberation chamber.



Figure 6.1. A Universal Software Radio Peripheral (USRP) from National Instruments.

As seen in Fig. 6.1, the USRP-2920 has two RF ports, clock input port, MIMO expansion slot, Gigabit Ethernet port, and power input. The circuit board of USRP is shown in Fig. 6.2 which consists of a mother board and a daughter board. The mother board provides basic functionalities such as power regulation, analog-to-digital conversion (ADC), digital-to-analog conversion (DAC), processor, and clock generation. The daughter board provides functionalities such as Digital Up Conversion (DUC), Digital Down Conversion (DDC), and signal conditioning. The USRP-2920 has a tunable RF transceiver and covers all important bands such as FM radio, GSM, GPS, radar, and ISM bands. Table 6.1 shows the technical specifications of USRP-2920 [42].

Building a simple communication system using the USRP is quite easy and requires only the basic understanding of its hardware and software, and we will briefly discuss these here. The USRP hardware is connected to a computer via Gigabit Ethernet cable from where it is controlled by the software. It has both the transmitter and the receiver chain on the same circuit board. The USRP hardware serves as an interface which accepts base-band input signals from the computer and outputs RF signal when used as a transmitter, and vice versa when used as a receiver. These

signals are transmitted and received using user-defined carrier frequency, sampling frequency, modulation and coding schemes, antenna configuration, amplifier gain, data, packet structure, and packet length. A complete transmitter and receiver chain of USRP-2920 together with its circuit board is shown in Fig. 6.2.

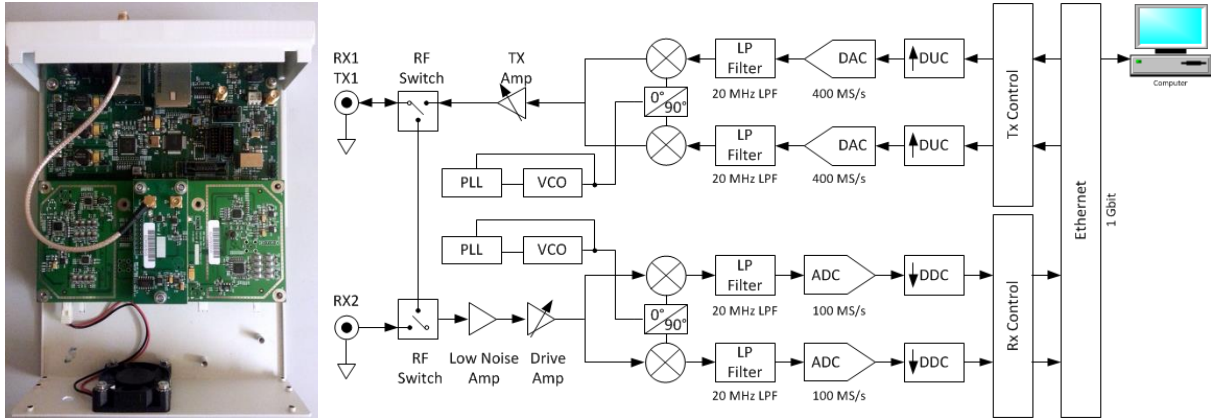


Figure 6.2. A circuit board (left) and a functional block diagram (right) of USRP-2920.

TABLE 6.1. TECHNICAL SPECIFICATIONS OF NI'S USRP

Characteristics	USRP-2920
Frequency of operation	50 MHz – 2.2 GHz
Typical maximum input power	0 dBm
Typical maximum output power	17-20 dBm (for 0.05 – 1.2 GHz), 15-18 dBm (for 1.2 – 2.2 GHz)
Digital-to-analog converter	2 channels, 400 MS/s, 16 bit
Analog-to-digital converter	2 channels, 100 MS/s, 14 bit

The USRP can be controlled by a variety of different software such as Matlab, GNU Radio, and LabVIEW. We chose NI's LabVIEW (short for Laboratory Virtual Instrument Engineering Workbench) because of better support from NI for USRP drivers. LabVIEW is a graphical programming language where different blocks are connected together by drawing wires between them. In Fig. 6.3, it is shown that a USRP is connected to a computer via Gigabit Ethernet interface, and a snapshot of LabVIEW based example code which implements USRP based transmitter. All the results in this chapter are based on USRP packet transmitter and packet receiver example code (available online at NI's webpage) with some minor modifications to serve the needs for our application.

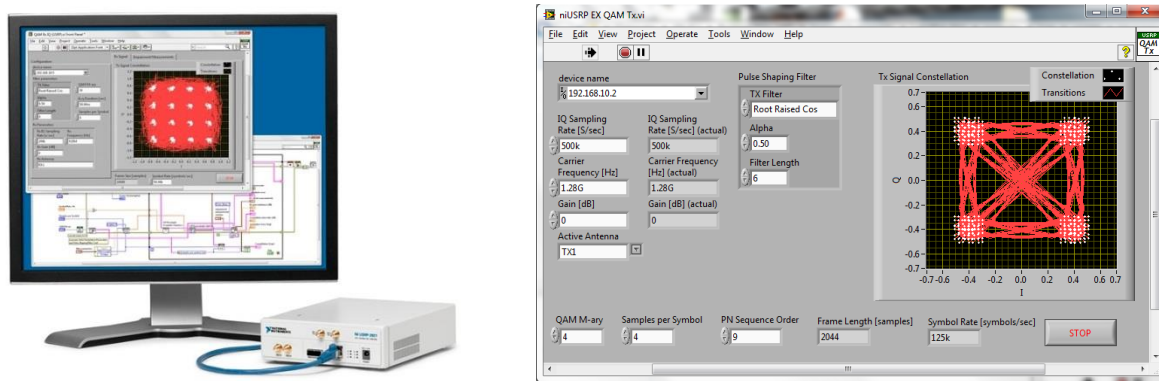


Figure 6.3. A USRP connected to a computer and controlled by LabVIEW (left), and a LabVIEW based GUI to control USRP transmitter (right).

The USRP packet transmitter converts the user defined data (e.g. text, image, audio, etc.) into binary format and packs the bits into packets. The packet structure is user defined which typically consists of guard bits, sync bits, packet number, data bits, and cyclic prefix. We use packet transmitter and packet receiver implemented in LabVIEW to establish a quick and reliable communication link between the transmitter and the receiver. The USRPs are connected to antennas inside reverberation chamber for OTA measurements as illustrated in Fig. 6.4 (left), and connected directly via cables for conducted measurements as illustrated in Fig. 6.4 (right). Packet Error Rate (PER) is measured at the receiver to determine the downlink performance of the communication system.

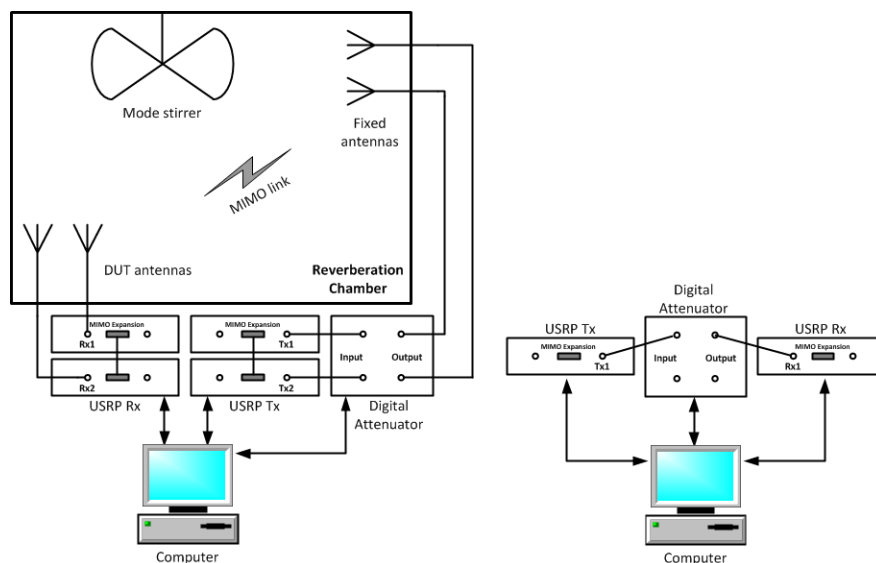


Figure 6.4. Illustration of MIMO OTA measurement setup inside reverberation chamber (left) and conducted measurement setup using cables (right).

In Fig. 6.4, the USRPs are connected to a digital attenuator to attenuate the USRP transmitter power. This is done in order to measure and compare the system performance at low power levels when PER is high. We will show some examples of active measurements (e.g. throughput, total radiated power, and total isotropic sensitivity) and passive measurements (e.g. efficiency, correlation, and diversity gain) using USRPs in combination with reverberation chamber.

We measured conducted throughput, shown in Fig. 6.5, to compare receiver threshold and downlink throughput of USRP at different carrier frequencies f_c (left) and at different sampling frequencies f_s (right). The results are shown in Fig. 6.5 where we observe a different throughput for different settings.

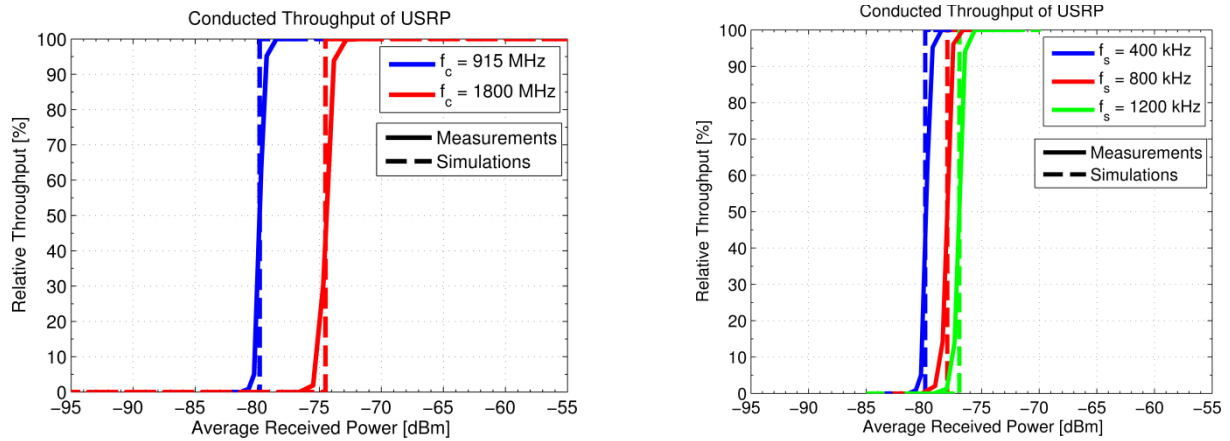


Figure 6.5. Conducted throughput of USRP for carrier frequency of 900 and 1800 MHz (left), and sampling frequency of 400, 800, and 1200 kHz (right).

We measure OTA throughput in reverberation chamber to compare different diversity combining schemes i.e. Selection Combining (SC) and Maximal Ratio Combining (MRC) and to compare SISO and MIMO antenna configurations. We observe in Fig. 6.6 (left) that MRC and SC combining schemes follow the ideal theoretical curves. Similarly, we observe in Fig. 6.6 (right) that MIMO and SISO throughput curves also have a good agreement with theory. The conducted and OTA throughput simulation results are based on the throughput model introduced in Chapter 4. The measured results show good agreement with simulated results.

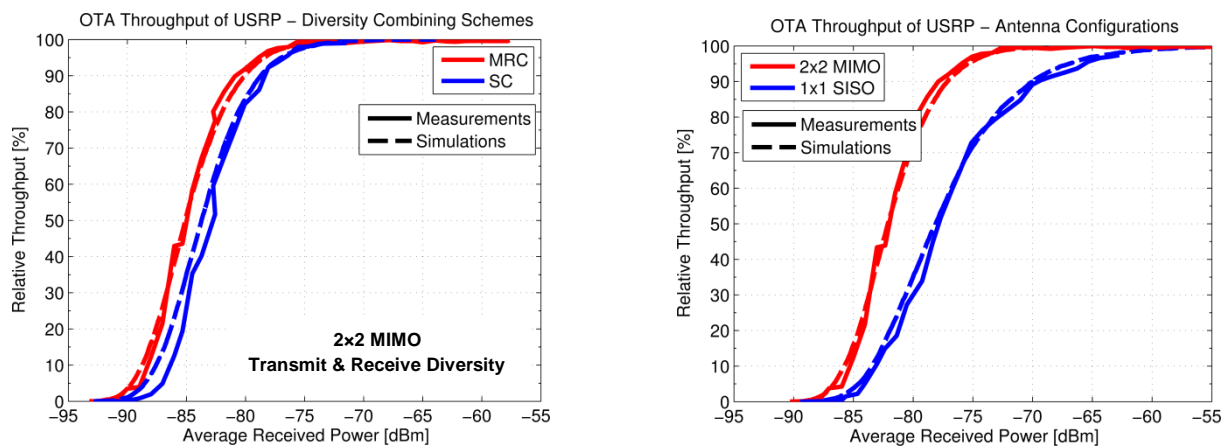


Figure 6.6. Comparison of OTA throughput of USRPs for MRC and SC diversity combining schemes (left) and for 1×1 SISO and 2×2 MIMO antenna configurations (right).

The Total Radiated Power (TRP) is a quality measure of a transmitter while Total Isotropic Sensitivity (TIS) is a quality measure of a receiver. In Fig. 6.7, we show measured TRP and TIS of a USRP for a frequency range of 600-2200 MHz, and the results show very good agreement with estimated results. We measured the TRP using the USRP as well as the Power Spectrum Analyzer

(PSA) and the results from both instruments agree very well. We measured the TIS of a 1×1 SISO system in flat fading, using two different methods (i) formal TIS measurement method [41], and (ii) newly suggested method [43] which uses OTA throughput. Again, the results show good agreement.

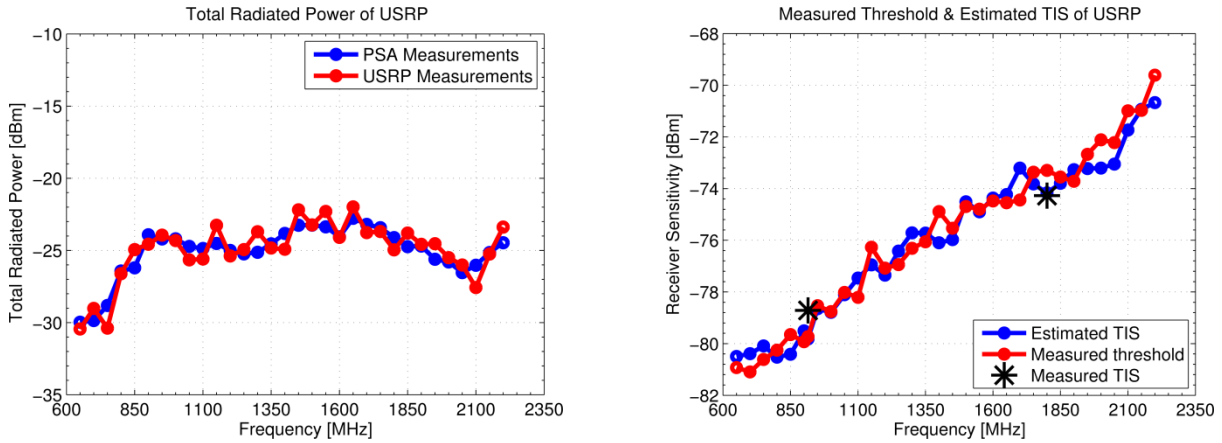


Figure 6.7. Total Radiated Power of USRP (left) and Total Isotropic Sensitivity of USRP (right).

Passive measurements using USRP inside reverberation chamber were also successful. Traditionally, for passive measurements we use Vector Network Analyzer (VNA) which is an expensive instrument. Nevertheless, VNA is able to measure reflected wave while USRP is not. Therefore, we can measure only high efficiency antennas using USRP, assuming that $S_{11} = 0$. In Fig. 6.8, we show antenna efficiency and correlation between two antennas can be measured by using USRPs in combination with the reverberation chamber. The results measured using VNA have fair agreement to the USRP measured results. The accuracy of the USRP measured results can be improved by further investigation.

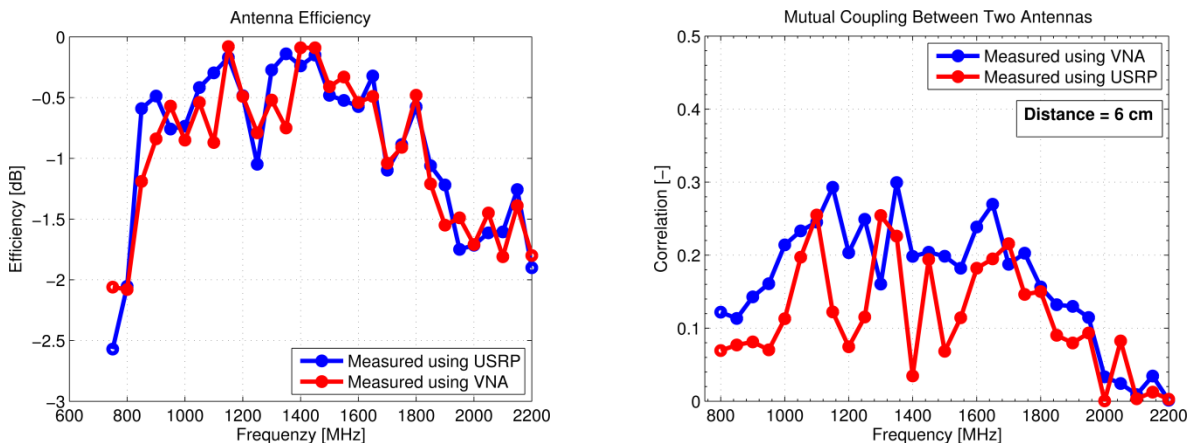


Figure 6.8. Single-port antenna efficiency (left) and correlation between two antenna ports (right) measured using VNA and USRP.

In short, the USRP is an inexpensive and flexible software radio platform. The shortcoming of the USRP-2920 are: (i) it is very time consuming to measure OTA performance using USRP compared to traditional measurement instruments available today, (ii) it is not a calibrated device, so it is necessary to calibrate it before using it to measure other wireless devices, (iii) the

frequency range is limited, and (iv) there is a power leakage between transmitter and receiver ports of a USRP and therefore it cannot be used in transceiver mode without any correcting measures. The new models of USRPs have improved performance which enables us to build larger and more complicated communication systems. These can also be tested in reverberation chamber in future.

CHAPTER

7

Characterization of Multiport Mobile Terminal

The performance characterization of single port mobile terminals has been studied a lot during the last decades. With the advancement in technology, LTE has become the latest standard for today's cellular communication systems. Unlike previous standards, LTE requires the use of multiple antennas inside the handset. The multiple antennas provide more possibilities to increase data throughput on a mobile phone but on the other hand it is challenging to accommodate more antennas in a limited space. A CST model of a practical two-port mobile phone mockup is shown in Fig. 7.1.

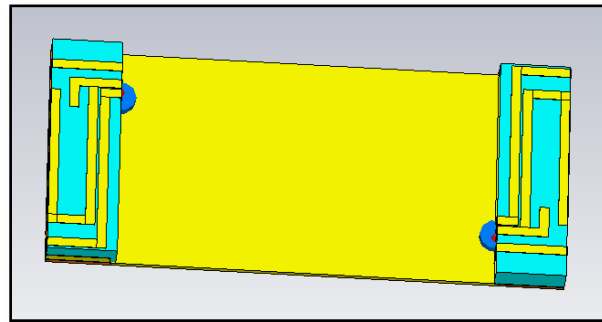


Figure 7.1. A model of two-port mobile phone in CST Microwave Studio.

The performance characterization of this practical mobile phone model is done using simulations in RIMP and random-LOS, and measurements in the reverberation chamber together with SAM head and hand phantom. This is done when the terminal is placed on both sides, i.e. right hand side (RHS) of the head and left hand side (LHS) of the head. The material properties of the head phantom are shown in Table 7.1.

TABLE 7.1. MATERIAL PROPERTIES OF HEAD PHANTOM

Material	Material Properties		
	ϵ'	ϵ''	μ
Head Phantom (Shell)	3.7	0.028	1
Head Phantom (Liquid)	41.33	16.91	1

The simulated S-parameters from CST are presented in Fig. 7.2. The two frequency bands of operation are 0.7-1.0 GHz & 1.7-3.2 GHz. The phone mockup is located on both sides, i.e., RHS and LHS, of the head according to the standardized talk positions, i.e., cheek position and tilt position.

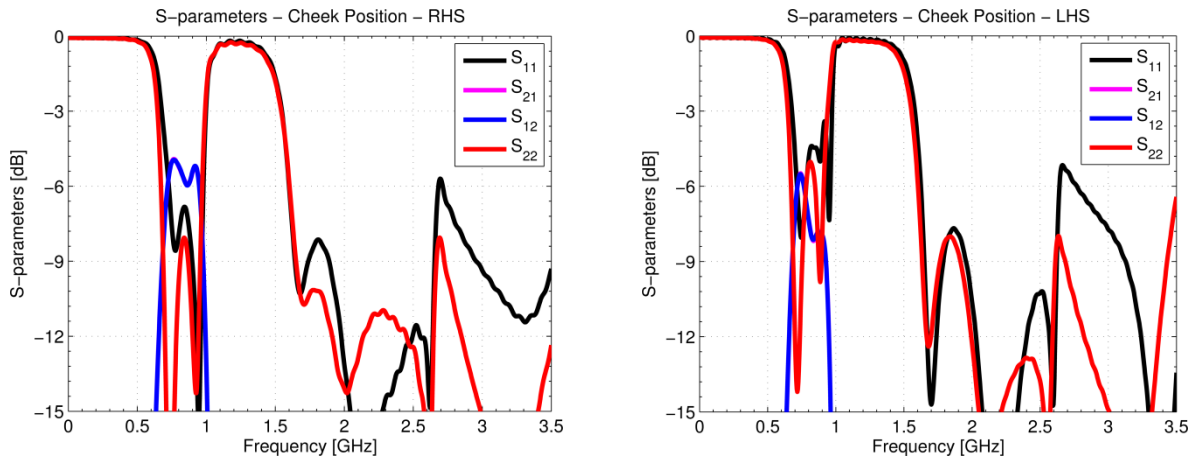


Figure 7.2. Simulated S-parameters of two-port mobile terminal in CST located on right (left) and left sides of the head (right) in the standard cheek position.

The simulated and measured diversity gains on both sides of the head in each talk position are shown in Fig. 7.3. From results it is observed that the measured and simulated diversity gains have good agreement in general with the exception of a few lower frequency points in the tilt position.

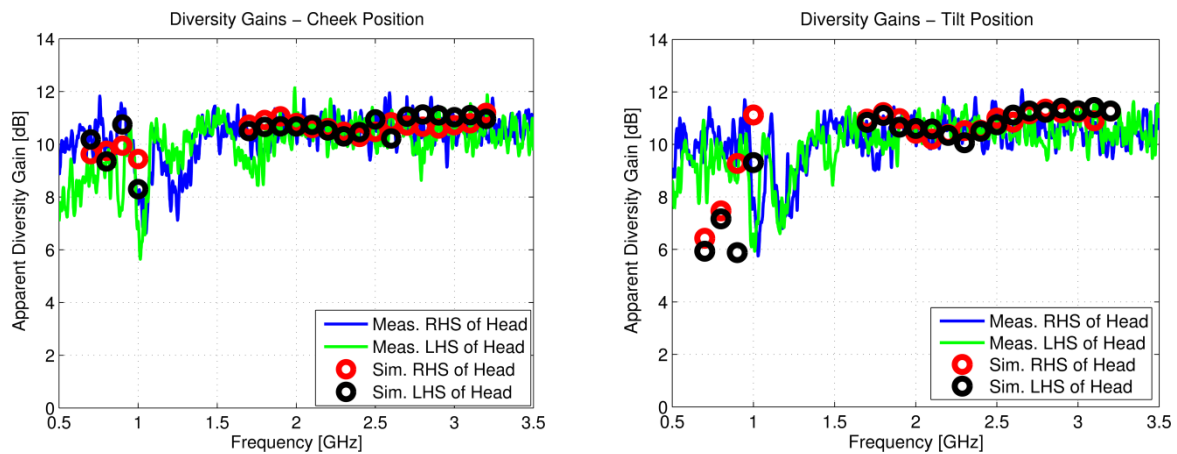


Figure 7.3. Measurements and simulations of diversity gains when two-port mobile terminal is on the right and left side of the head for cheek position (left) and tilt position (right).

The study of correlation between far-field patterns, in paper [D2], on both sides of the head is done using the same two-port mobile phone mockup (see Fig. 7.1) which is simulated in CST Microwave Studio. The purpose of the study is to characterize the performance in LOS environment when using the mobile phone on right side and left side of the head. The study shows that the correlation between the far-field patterns on both sides of the head depends on the chosen coordinate system. The correlation is approximately 1 (i.e. high correlation) when the

far-field patterns are presented in the co-ordinate system fixed to the mobile phone. The same patterns show the correlation of approximately 0 (i.e. no correlation) when they are presented in the co-ordinate system fixed to the environment. From Fig. 7.4, we can see that UVW co-ordinate system which is fixed to the head (or environment) is the same on both sides of the head. The XYZ co-ordinate system which is fixed to the mobile phone has a difference of 90-degrees i.e. vertical direction on one side of the head becomes horizontal on the other side and vice versa. In multipath environments such as RIMP, the position, orientation, and shape of the radiation pattern does not affect the performance. In other environments such as random-LOS, the shape of the radiation pattern does have a strong impact on the performance.

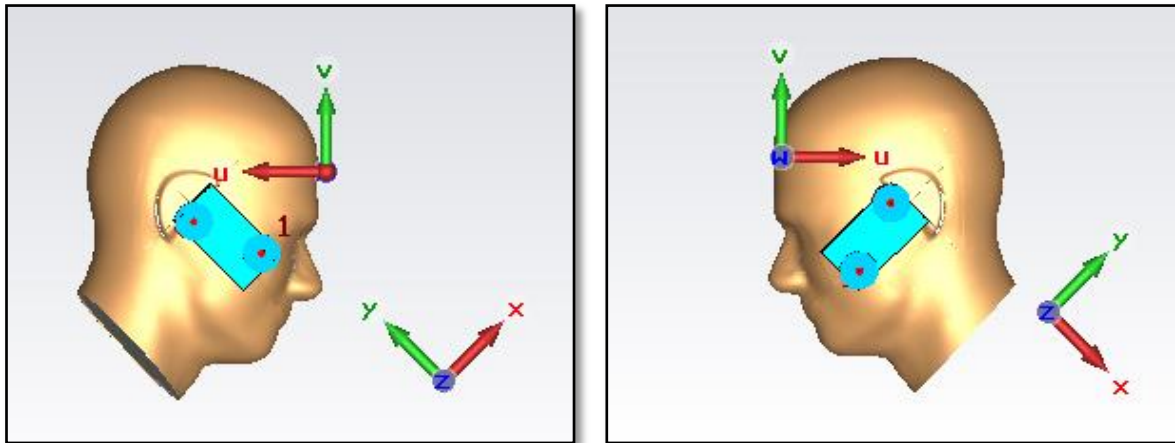


Figure 7.4. A model of two-port mobile phone mockup with SAM head phantom in CST Microwave Studio showing XYZ and UVW coordinate systems.

The correlation between far-field patterns on both sides of the head is presented together with the effect of SAM head and hand phantom, and only with the head phantom in Figs. 7.5 and 7.6.

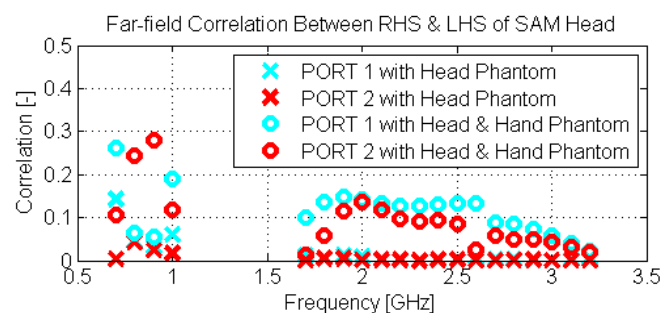


Figure 7.5. Magnitude of complex correlation between far-field functions on the right and left sides of the head when the coordinate system is aligned to the environment i.e. UVW coordinate system.

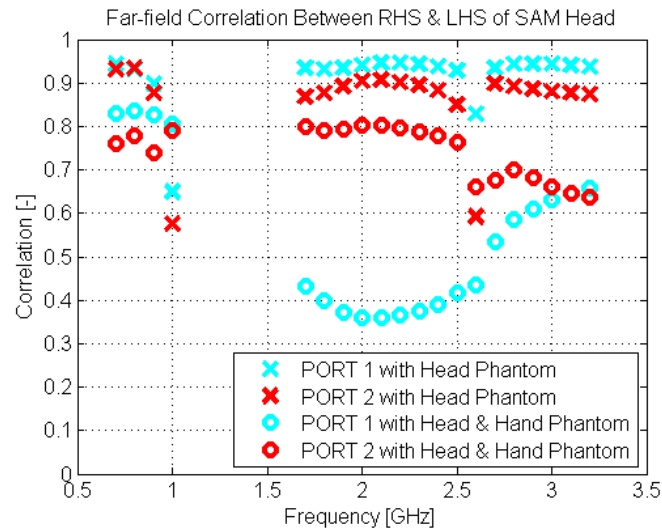


Figure 7.6. Magnitude of complex correlation between far-field functions on the right and left sides of the head when the coordinate system is aligned to the terminal i.e. XYZ coordinate system.

The correlation between the far-field patterns for port 1, with head and hand phantom in Fig. 7.6, shows deviation which is clearly due to the position of fingers affecting the pattern differently. The results for port 2 are not affected because they are covered by the hand palm on both sides in approximately the same way.

Recently, an ultra-wideband (UWB) bow-tie antenna has been developed at Chalmers University of Technology, Sweden. It is a four-port antenna which is an extension of self-grounded bow-tie antenna shown in [32]. It is named bow-tie antenna after its shape which has a resemblance to a bow-tie. The details of design and developments of this antenna and using genetic algorithms for optimization are shown in [33, 34]. A compact size UWB multiport antenna with very low mutual coupling between the antenna ports brings with itself a lot of possible applications and interests in research and development for wireless MIMO communication systems. For example, the antenna can be used in WiFi, LTE base station, etc. The CST model of the UWB four-port bow-tie antenna is shown in Fig. 8.1.

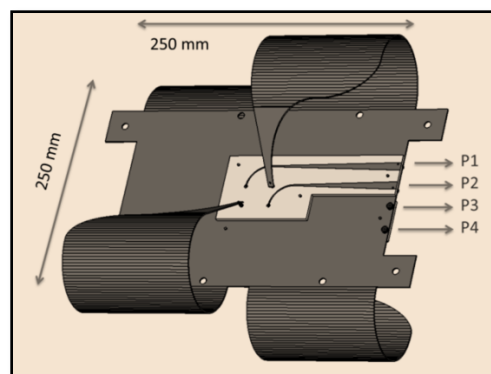


Figure 8.1. CST model of four-port self-grounded bow-tie antenna.

The performance of bow-tie antenna in terms of S-parameters is shown in Fig. 8.2. These S-parameters are obtained from electromagnetic simulations of this prototype antenna in CST Microwave Studio. The operating frequency range for this UWB antenna is 0.5-16 GHz. It has high embedded radiation efficiency and low correlation between the antenna ports. The embedded radiation efficiency is defined in [7]. The formulas in terms of S-parameters for embedded radiation efficiency $e_{rad,i}$ and total embedded radiation efficiency $e_{rad,i\,total}$ of embedded element number i when there are total N elements and no ohmic losses, are shown below in (8.1) and (8.2) respectively:

$$e_{rad,i} = \frac{1 - \sum_{j=1}^N |S_{ij}|^2}{1 - |S_{ii}|^2} ; e_{refl,i} = 1 - |S_{ii}|^2 \quad (8.1)$$

$$e_{rad,i,total} = e_{rad,i} \times e_{refl,i} = 1 - \sum_{j=1}^N |S_{ij}|^2 \quad (8.2)$$

where $e_{refl,i}$ denotes mismatch efficiency. Since all antenna petals are symmetrical or anti-symmetrical with respect to each other, they have similar radiation efficiency as shown in Fig. 8.3.

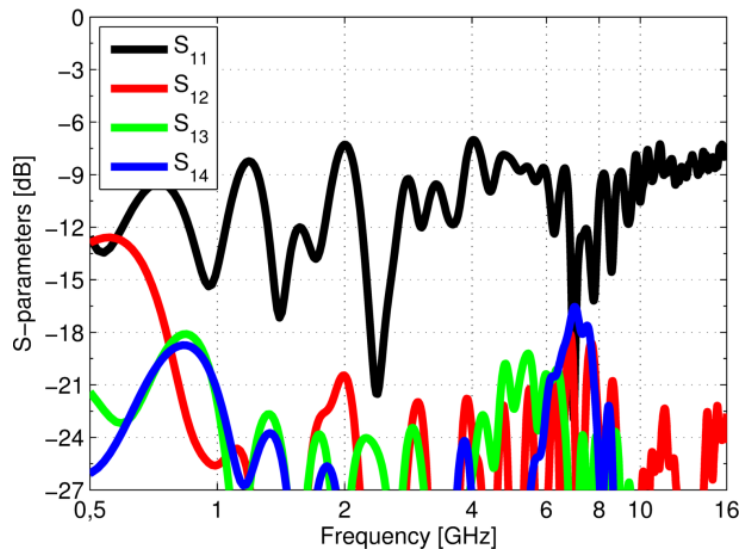


Figure 8.2. Simulated S-parameters of 4-port self-grounded bow-tie antenna from CST.

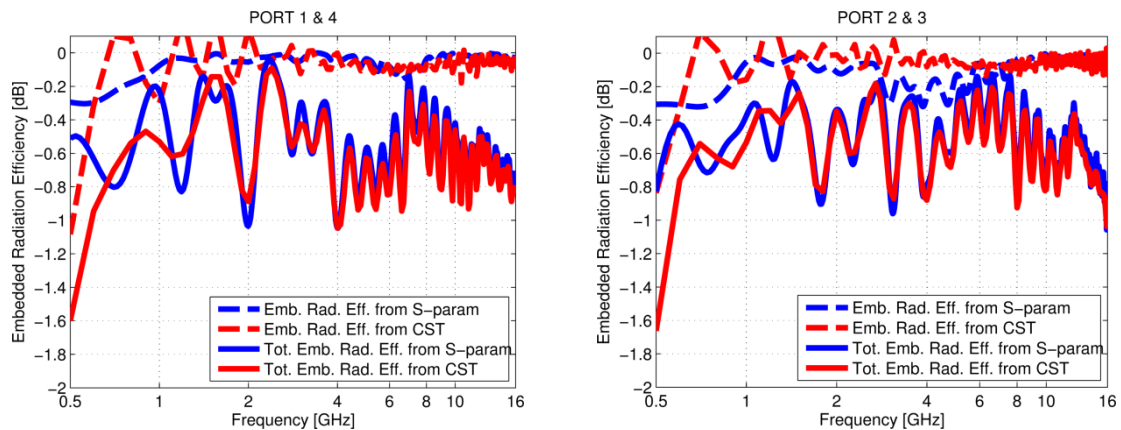


Figure 8.3. Embedded radiation efficiencies of ports 1 & 4 (left) and ports 2 & 3 (right) calculated by CST (red color) and calculated by S-parameters from CST (blue color).

The correlation between the ports in a RIMP environment is very low, i.e. smaller than 0.1, as shown by simulated results in Fig. 8.4. The results are verified by measurements in a reverberation chamber, see paper [E1]. This is due to the fact that mutual coupling between the ports is lower than -10 dB as shown in Fig. 8.2. The correlation between the antenna ports can be calculated by using far-field functions [7] or S-parameters[44]. The formula for calculating correlation ρ in terms of S-parameters for an antenna with no ohmic losses is shown in (8.3).

$$\rho_{ij} = \frac{S_{ii}S_{ij} + S_{ji}S_{jj}}{\sqrt{[1 - (|S_{ii}|^2 + |S_{ij}|^2)][1 - (|S_{ji}|^2 + |S_{jj}|^2)]}} \quad (8.3)$$

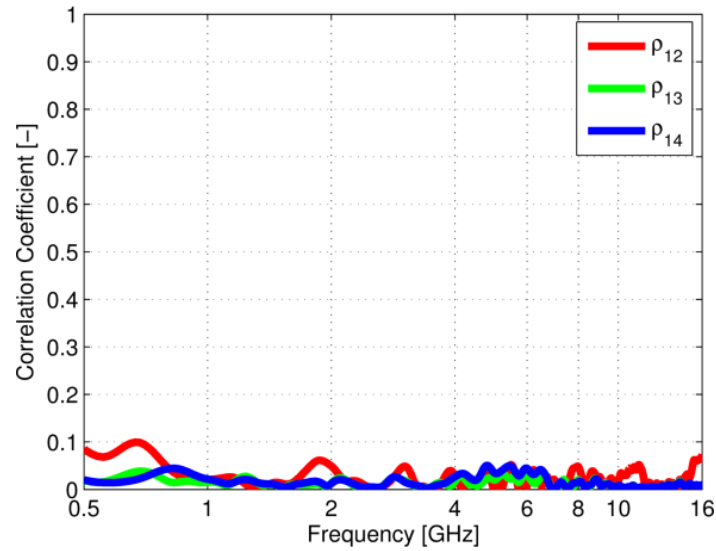


Figure 8.4. Magnitude of complex correlations between port 1 and port 2, 3, and 4 using S-parameters.

The CDFs of each antenna port and MRC-combined diversity channels in a RIMP environment for the whole frequency of operation are plotted in Fig. 8.5. The diversity gains are calculated at 1% CDF-level from Fig. 8.5 and plotted in Fig. 8.6 which shows that there is a clear improvement in the diversity gains for the whole frequency range of the antenna when we increase the spatial diversity from 2-port to 3-port and 4-port diversity antenna. The improvement is seen over the whole wide bandwidth, which makes this antenna very useful for many practical applications.

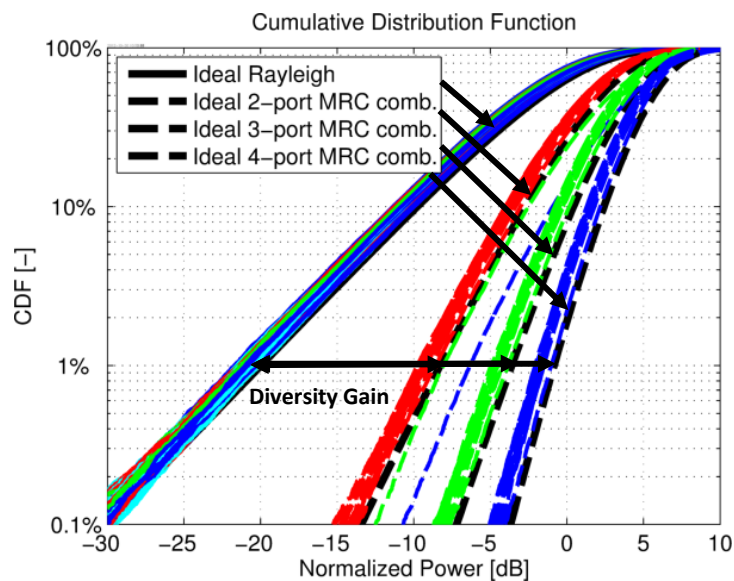


Figure 8.5. CDFs of each antenna port and 2, 3, and 4-port MRC-combined diversity channel

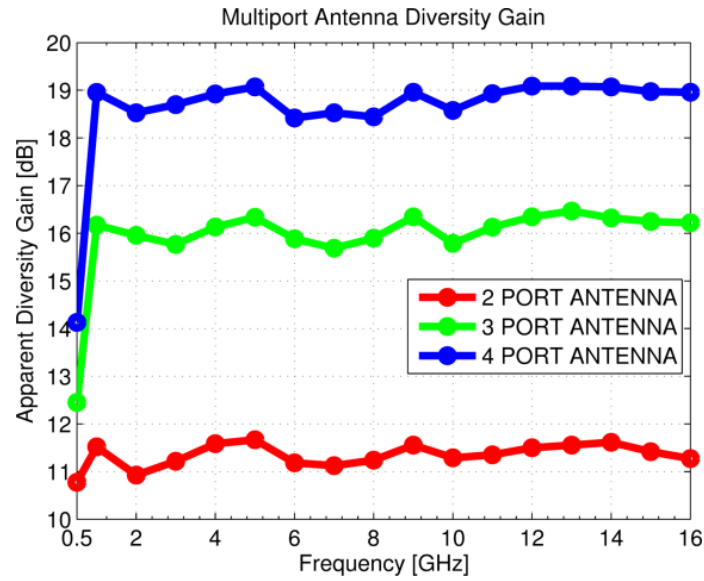


Figure 8.6. Apparent diversity gains at 1% CDF-level for 2, 3, and 4-port diversity antenna in RIMP environment.

The antenna diversity gain is quite close to the ideal MRC-combined 2-port, 3-port, and 4-port diversity antennas i.e. 11.7 dB, 16.4 dB, and 19.1 dB respectively. This is due to the very high embedded radiation efficiencies (see Fig. 8.3), and very low cross-correlations between the antenna-ports (see Fig. 8.4). The low apparent diversity gain at 0.5 GHz is partly due to lower total embedded radiation efficiencies and higher correlation, and partly due to not very accurate simulated far-field patterns at this frequency. This can be further investigated and improved. A comparison of the simulated and the measured apparent diversity gain can be seen in paper [E1].

CHAPTER Simulation Tools

9

Simulation tools are quite essential to test new ideas e.g. random-LOS channel model, and to validate established ideas e.g. RIMP channel model. They provide cost effective method to convey useful information in a pedagogical way. At Chalmers University, we have developed two multipath simulators i.e. Rayleigh Lab and Visual Random Multipath Lab (ViRM Lab). Both simulators are developed in MATLAB and are open source. The graphical user interface (GUI) of Rayleigh Lab is shown in Fig. 9.1.

The Rayleigh Lab is based on random number generator in MATLAB. The purpose of this tool is to simulate the response (i.e. complex voltage samples) on the antenna ports in RIMP environment i.e. Rayleigh fading channels. It is already known that the channel in RIMP environment is independent of the shape of the far-field radiation pattern and the orientation and position of the antenna. Therefore, it is easier to simulate complex Gaussian distributed channels using random number generator instead of using far-field patterns and simulating RIMP environment.

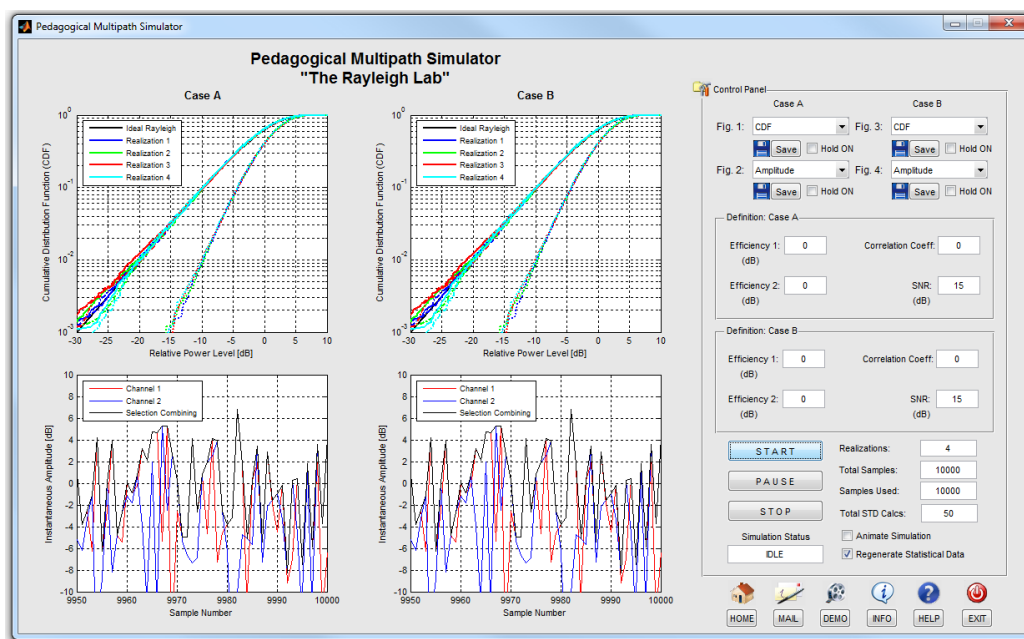


Figure 9.1. The GUI of Rayleigh Lab – a pedagogical multipath simulator.

The Rayleigh Lab simulates an array of complex voltage samples at each antenna port in a Rayleigh fading environment. The distribution of these voltage samples is complex Gaussian. The different channels on each antenna port are combined using either SC or MRC combining

scheme. It is a simple pedagogical tool for studying convergence using random numbers. We can study convergence of radiation efficiency, correlation, diversity gain, and capacity of a MIMO system. The simulation tool provides a user-friendly GUI, as shown in Fig. 9.1. The GUI allows user to input values for different parameters e.g. embedded element efficiencies and correlation to calculate diversity gain and capacity. Two different cases can be compared side-by-side based on the user-inputs. The study of standard deviation in the measurements of efficiency, diversity gain, and capacity can also be performed using Rayleigh-lab.

The ViRM Lab is a ray-based simulation tool which is also developed in MATLAB. This tool uses antenna far-field patterns and simulates RIMP environment using isotropically distributed incoming waves towards these far-field patterns with random angle-of-arrival. Different studies including the comparison of 2D and 3D multipath environments, and performance characterization in random-LOS are accomplished using this tool. The far-field patterns from different electromagnetic simulation software such as CST Microwave Studio and High Frequency Structural Simulator (HFSS), and measured patterns from anechoic chamber can be imported into ViRM Lab. The procedure to run a simulation using functions built in ViRM Lab can be explained better by the flowchart shown in Fig. 9.2.

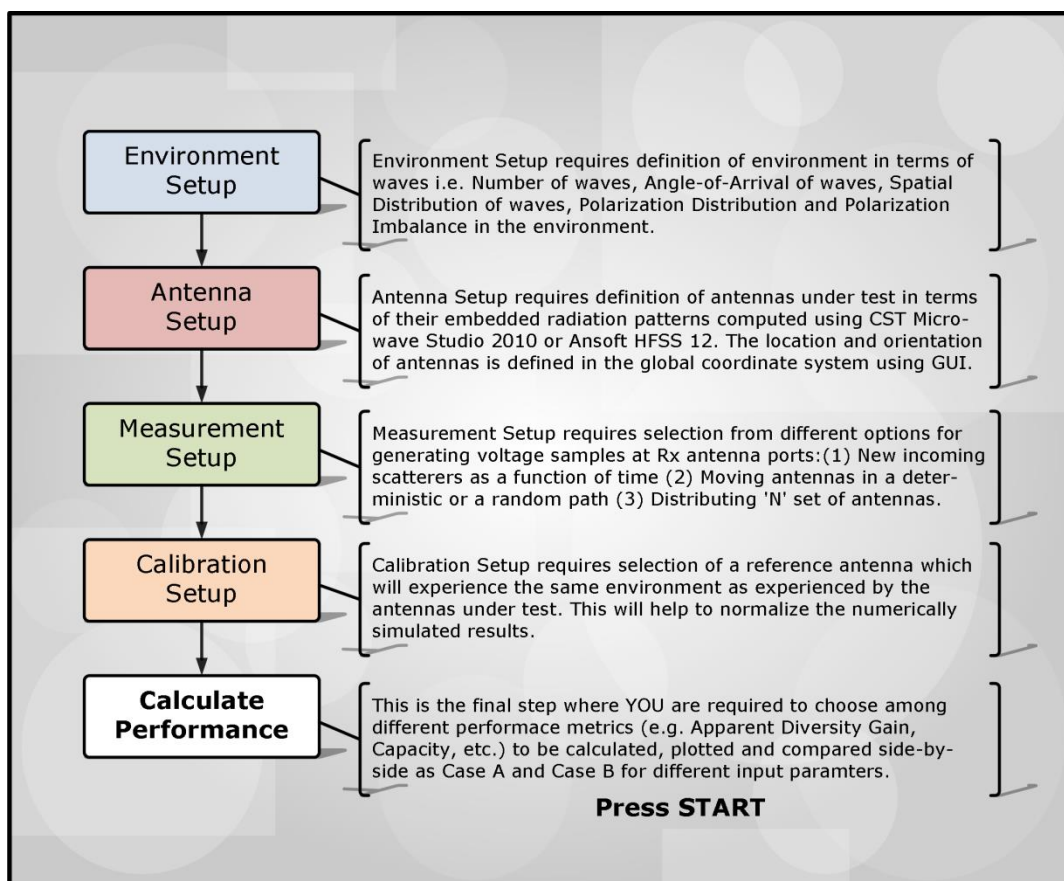


Figure 9.2. Flow chart of a ray-based multipath simulation tool – ViRM Lab.

Firstly, the environment or the channel model is defined in which the antenna is present, e.g. RIMP, random-LOS, etc. An environment is setup by defining number of incoming waves, AoA

and distribution of AoA of these waves, polarization, and amplitude and phase of the incoming waves.

Secondly, antenna setup is performed by loading the measured or simulated embedded far-field pattern(s) of the antenna into ViRM Lab. The location(s) and the orientation(s) of the antenna(s) are also user-defined i.e. either fixed or random.

Thirdly, the simulation setup is defined by defining the number of complex voltage samples to be simulated on each antenna port of a multiport antenna. The number of samples can be a function of (i) time, (ii) space, i.e. fixed or random positions and orientations of the antenna, or (iii) number of antennas.

Fourthly, the simulated complex voltage samples at the antenna ports are calibrated by normalization e.g. by using isotropic antenna as a reference antenna for calibration.

Finally, a performance metric of interest e.g. efficiency, correlation, diversity gain, capacity, or throughput can be chosen for performance evaluation. This can help us to (i) compare performance of the same antenna in different environments e.g. 2D and 3D multipath environments, and (ii) compare performance of different antennas in the same environments e.g. dipoles and pencil-beams in RIMP environment.

CHAPTER Conclusion & Future Work

10

This thesis is a compilation of results and discussions on the following topics: using rich isotropic multipath environment as a reference environment for OTA characterization of small antennas and mobile devices in multipath; using randomness of the users in terms of random positions and orientations of hand-held devices in pure-LOS environment; using simple theoretical models to estimate OTA throughput, PoD, and TIS of wireless devices with MIMO and OFDM; and using simulation tools to validate measurements. In short, this thesis provides arguments in favor of using RIMP and random-LOS as two extreme reference environments for the characterization of mobile wireless terminals. These arguments are supported very well by simulations and measurements. At the time of writing this thesis, there is not a single channel model that can define all possible environments for mobile wireless devices including user randomness. The results in this thesis provide evidence that RIMP is a good reference environment for measuring mobile devices in multipath. RIMP provides a unique value for radiation efficiency, diversity gain, and channel capacity, and it is independent of the position and orientation of the terminal in the environment. Furthermore, the pure-LOS environment appears to be random in three-dimensional space when considering all possible positions and orientations of the wireless terminal. Fig. 10.1 illustrates the randomness of the orientation of the mobile wireless terminals. Our hypothesis states that:

“If a wireless device is tested with good performance in both pure-LOS and RIMP environments, it will also perform well in real-life environments and situations, in a statistical sense [31].”



Figure 10.1. Illustration of random orientations of mobile wireless devices e.g. iPad

While some work has already been done, in the scope of this thesis, to characterize the performance of wireless devices and antennas in multipath environments, there are still many interesting investigations left to be done in future. For example, using USRPs in multi-user MIMO, massive MIMO, and random-LOS applications are few of the most interesting projects. Such studies are of great value and interest to progress towards more advance problems in wireless research.

Bibliography

- [1] P. Kildal, C. Orlenius, and J. Carlsson, "OTA testing in multipath of antennas and wireless devices with MIMO and OFDM," *Proceedings of the IEEE*, vol. 100, pp. 2145-2157, 2012.
- [2] J. Carlsson, U. Carlberg, A. Hussain, and P. Kildal, "About measurements in reverberation chamber and isotropic reference environment," in *20th International Conference on Applied Electromagnetics and Communications (ICECom)*, 2010, p. 4 pp.
- [3] X. Chen, P. Kildal, and J. Carlsson, "Comparisons of different methods to determine correlation applied to multi-port UWB eleven antenna," in *Proceedings of the 5th European Conference on Antennas and Propagation (EUCAP)*, 2011, pp. 1776-1780.
- [4] X. Chen, P. S. Kildal, and J. Carlsson, "Measurement uncertainties of capacities of multi-antenna system in anechoic chamber and reverberation chamber," in *8th International Symposium on Wireless Communication Systems (ISWCS)*, 2011, pp. 216-220.
- [5] X. Chen, P. S. Kildal, J. Carlsson, and Y. Jian, "Comparison of ergodic capacities from wideband MIMO antenna measurements in reverberation chamber and anechoic chamber," *IEEE Antennas and Wireless Propagation Letters*, vol. 10, pp. 446-449, 2011.
- [6] X. Chen, P. Kildal, J. Carlsson, and Y. Jian, "MRC diversity and MIMO capacity evaluations of multi-port antennas using reverberation chamber and anechoic chamber," *IEEE Transactions on Antennas and Propagation*, vol. 61, pp. 917-926, 2013.
- [7] K. Rosengren and P. S. Kildal, "Radiation efficiency, correlation, diversity gain and capacity of a six-monopole antenna array for a MIMO system: theory, simulation and measurement in reverberation chamber," *IEE Proceedings - Microwaves, Antennas and Propagation*, vol. 152, pp. 7-16, 2005.
- [8] P. S. Kildal and K. Rosengren, "Correlation and capacity of MIMO systems and mutual coupling, radiation efficiency, and diversity gain of their antennas: simulations and measurements in a reverberation chamber," *IEEE Communications Magazine*, vol. 42, pp. 104-112, 2004.
- [9] C. L. Holloway, H. A. Shah, R. J. Pirkl, W. F. Young, D. A. Hill, and J. Ladbury, "Reverberation chamber techniques for determining the radiation and total efficiency of antennas," *IEEE Transactions on Antennas and Propagation*, vol. 60, pp. 1758-1770, 2012.
- [10] P. S. Kildal and K. Rosengren, "Electromagnetic analysis of effective and apparent diversity gain of two parallel dipoles," *IEEE Antennas and Wireless Propagation Letters*, vol. 2, pp. 9-13, 2003.
- [11] J. H. Rudander, K. Ikram e, P. S. Kildal, and C. Orlenius, "Measurements of RFID tag sensitivity in reverberation chamber," *IEEE Antennas and Wireless Propagation Letters*, vol. 10, pp. 1345-1348, 2011.
- [12] C. Orlenius, C. L. Patane, A. Skarbratt, J. Asberg, and M. Franzen, "Analysis of MIMO OTA measurements for LTE terminals performed in reverberation chamber," in *6th European Conference on Antennas and Propagation (EUCAP)*, 2012, pp. 1934-1938.
- [13] P. Kildal, A. Hussain, G. Durisi, C. Orlenius, and A. Skarbratt, "LTE MIMO multiplexing performance measured in reverberation chamber and accurate simple theory," in *6th European Conference on Antennas and Propagation (EUCAP)*, 2012, pp. 2299-2302.
- [14] A. Hussain, P. Kildal, and G. Durisi, "Modeling system throughput of single and multi-port wireless LTE devices," in *IEEE Antennas and Propagation Society International Symposium*, 2012.
- [15] P. Kildal, A. Hussain, X. Chen, C. Orlenius, A. Skarbratt, J. Asberg, *et al.*, "Threshold receiver model for throughput of wireless devices with MIMO and frequency diversity measured in reverberation chamber," *IEEE Antennas and Wireless Propagation Letters*, vol. 10, pp. 1201-1204, 2011.

- [16] A. Hussain and P. Kildal, "Study of OTA throughput of LTE terminals for different system bandwidths and coherence bandwidths," in *7th European Conference on Antennas and Propagation (EuCAP)*, 2013, pp. 312-314.
- [17] X. Chen and P. S. Kildal, "Accuracy of antenna input reflection coefficient and mismatch factor measured in reverberation chamber," in *3rd European Conference on Antennas and Propagation (EuCAP)*, 2009, pp. 2678-2681.
- [18] A. Hussain, U. Carlberg, J. Carlsson, and P. S. Kildal, "Analysis of statistical uncertainties involved in estimating ergodic MIMO capacity and diversity gain in Rayleigh fading environment," in *20th International Conference on Applied Electromagnetics and Communications (ICECom)*, 2010, pp. 1-4.
- [19] X. Chen and P.-S. Kildal, "Frequency-dependent effects of platform and wall antennas on measurement uncertainty in reverberation chamber," in *Proceedings of the Fourth European Conference on Antennas and Propagation (EuCAP)*, 2010, pp. 1-3.
- [20] J. Carlsson, A. Wolfgang, C. Orlenius, and P. S. Kildal, "Accuracy of radiation efficiency measurements in a reverberation chamber," in *Antenn 03. Nordic Antenna Symposium*, Arboga, Sweden, 2003, pp. 297-302.
- [21] E. Engvall, C. L. Holloway, J. M. Ladbury, and P. S. Kildal, "A study of uncertainty models in a reverberation chamber at NIST," in *IEEE Antennas and Propagation Society International Symposium (APSURSI)*, 2012, pp. 1-2.
- [22] P. Kildal, L. Sz-Hau, and X. Chen, "Direct coupling as a residual error contribution during OTA measurements of wireless devices in reverberation chamber," in *IEEE International Symposium on Antennas & Propagation & USNC/URSI National Radio Science Meeting*, Piscataway, NJ, USA, 2009, p. 4 pp.
- [23] P. Kildal, X. Chen, C. Orlenius, M. Franzen, and C. S. L. Patane, "Characterization of reverberation chambers for OTA measurements of wireless devices: physical formulations of channel matrix and new uncertainty formula," *IEEE Transactions on Antennas and Propagation*, vol. 60, pp. 3875-3891, 2012.
- [24] A. Hussain, P. S. Kildal, and J. Carlsson, "Uncertainties in estimating ergodic MIMO capacity and diversity gain of multipoint antenna systems with different port weights," in *Proceedings of the 5th European Conference on Antennas and Propagation (EUCAP)*, 2011, pp. 310-314.
- [25] X. Chen, P. S. Kildal, and L. Sz-Hau, "Estimation of average Rician K-factor and average mode bandwidth in loaded reverberation chamber," *IEEE Antennas and Wireless Propagation Letters*, vol. 10, pp. 1437-1440, 2011.
- [26] X. Chen, P. S. Kildal, C. Orlenius, and J. Carlsson, "Channel sounding of loaded reverberation chamber for over-the-air testing of wireless devices: coherence bandwidth versus average mode bandwidth and delay spread," *IEEE Antennas and Wireless Propagation Letters*, vol. 8, pp. 678-681, 2009. See also correction in Vol. 12, 2013.
- [27] X. Chen and P. S. Kildal, "Theoretical derivation and measurements of the relationship between coherence bandwidth and RMS delay spread in reverberation chamber," in *3rd European Conference on Antennas and Propagation (EuCAP)*, 2009, pp. 2687-2690.
- [28] A. Hussain, P. S. Kildal, U. Carlberg, and J. Carlsson, "Diversity gains of multipoint mobile terminals in multipath for talk positions on both sides of the head," in *7th European Conference on Antennas and Propagation (EuCAP)*, 2013, pp. 863-866.
- [29] "IEEE recommended practice for determining the peak spatial-average specific absorption rate (SAR) in the human head from wireless communications devices: measurement techniques," *IEEE Std 1528-2003*, pp. 1-149, 2003.
- [30] A. Hussain, P. Kildal, U. Carlberg, and J. Carlsson, "Correlation between far-field patterns on both sides of the head of two-port antenna on mobile terminal," presented at the IEEE Antennas and Propagation Society International Symposium (APSURSI), 2013.
- [31] P. Kildal and J. Carlsson, "New approach to OTA testing: RIMP and pure-LOS reference environments & a hypothesis," in *7th European Conference on Antennas and Propagation (EuCAP)*, Gothenburg, 2013, pp. 315-318.

- [32] Y. Jian and A. Kishk, "A novel low-profile compact directional ultra-wideband antenna: the self-grounded bow-tie antenna," *IEEE Transactions on Antennas and Propagation*, vol. 60, pp. 1214-1220, 2012.
- [33] A. Al-Rawi, "A new compact wideband MIMO antenna for reverberation chambers," Master of Science Thesis, Signals & Systems, Chalmers University of Technology, Gothenburg, 2012.
- [34] A. Al-Rawi, A. Hussain, J. Yang, M. Franzen, C. Orlenius, and A. A. Kishk, "A new compact wideband MIMO antenna - the double-sided tapered self-grounded monopole array," *IEEE Transactions on Antennas and Propagation*, vol. 62, pp. 3365-3369, 2014.
- [35] A. Hussain, P. Kildal, A. Al-Rawi, and J. Yang, "Efficiency, correlation, and diversity gain of UWB multiport self-grounded bow-tie antenna in rich isotropic multipath environment," in *International Workshop on Antenna Technology (iWAT)*, 2013, pp. 336-339.
- [36] P. Kildal, A. Hussain, U. Carlberg, and C. Carlsson, "On using isotropic multipath as reference environment for OTA performance: Uncertainty due to convergence of statistical expectation when estimating ergodic capacity and diversity gain," presented at the European Cooperation in the field of Scientific and Technical Research - COST2100, Alborg, 2010.
- [37] U. Carlberg, J. Carlsson, A. Hussain, and P. S. Kildal, "Ray based multipath simulation tool for studying convergence and estimating ergodic capacity and diversity gain for antennas with given far-field functions," in *20th International Conference on Applied Electromagnetics and Communications (ICECom)*, 2010.
- [38] M. Godavarti, T. L. Marzetta, and S. Shamai, "Capacity of a mobile multiple-antenna wireless link with isotropically random Rician fading," *IEEE Transactions on Information Theory*, vol. 49, pp. 3330-3334, 2003.
- [39] A. Hussain, P. Kildal, U. Carlberg, and J. Carlsson, "About Random LOS in Rician Fading Channels for MIMO OTA Tests," presented at the 2011 International Symposium on Antennas and Propagation (ISAP 2011) Jeju, 2011.
- [40] P. Kildal, U. Carlberg, and J. Carlsson, "Definition of antenna diversity gain in user-distributed 3D-random line-of-sight," *Journal of electromagnetic engineering and science*, vol. 13, pp. 86-92, 2013.
- [41] C. Orlenius, P. S. Kildal, and G. Poilasne, "Measurements of total isotropic sensitivity and average fading sensitivity of CDMA phones in reverberation chamber," in *IEEE Antennas and Propagation Society International Symposium*, 2005, pp. 409-412 Vol. 1A.
- [42] National Instruments Corporation. Available: <http://www.ni.com>
- [43] A. Hussain and P. Kildal, "Replacing TIS by OTA throughput for measuring receiver quality of SISO & MIMO LTE terminals in reverberation chambers," *manuscript submitted to IEEE Transactions on Antennas and Propagations*, June 2014.
- [44] J. S. Colburn, Y. Rahmat-Samii, M. A. Jensen, and G. J. Pottie, "Evaluation of personal communications dual-antenna handset diversity performance," *IEEE Transactions on Vehicular Technology*, vol. 47, pp. 737-746, 1998.

Part II
Publications

